INTERNATIONAL ATOMIC ENERGY AGENCY
UNITED NATIONS EDUCATIONAL, SCIENTIFIC AND CULTURAL ORGANIZATION

INTERNATIONAL CENTRE FOR THEORETICAL PHYSICS
34100 TRIESTE (ITALY) - P.O.B. 586 - MIRAMARE - STRADA COSTIERA 11 - TELEPHONE: 2240-1
CABLE: CENTRATOM - TELEX 460392-1

H4.SMR/303 - 32

WORKSHOP
GLOBAL GEOPHYSICAL INFORMATICS WITH APPLICATIONS TO RESEARCH IN EARTHQUAKE PREDICTIONS AND REDUCTION OF SEISMIC RISK

(15 November - 16 December 1988)

THE ROLE OF TIME DELAYS IN PRODUCING INSTABILITY ENGINEERING MODEL OF SEISMIC RISK

L. KNOPOFF

University of California
Los Angeles
U.S.A.

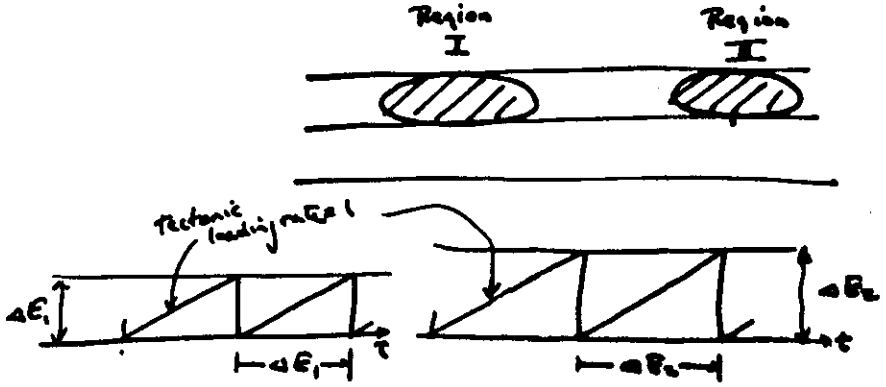

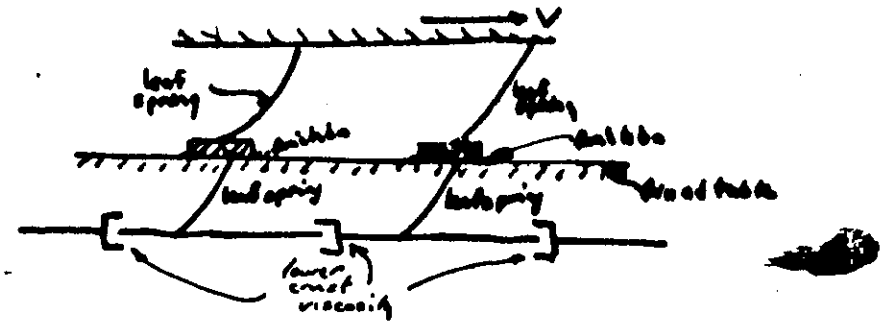

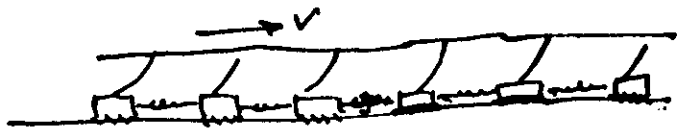

Burridge & Knopoff (1967)

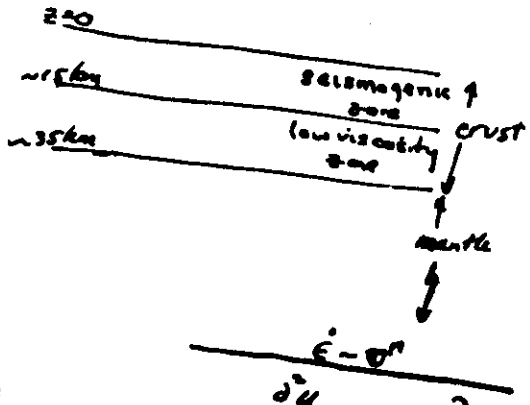

$\dot{\epsilon} \sim \sigma^n$ $\quad n \sim 3$ to 3.5

$$\left.\begin{aligned} \frac{\partial^2 u}{\partial x\,\partial t} &= K\sigma^n \\ \frac{\partial \sigma}{\partial x} &= \rho \frac{\partial^2 u}{\partial t^2} \end{aligned}\right\} \Rightarrow \frac{\partial^2 \sigma}{\partial x^2} = K\rho \frac{\partial \sigma^n}{\partial t}$$

$$\text{or} \quad \frac{\partial^2 \dot{u}^n}{\partial x^2} = (K\rho)^n \frac{\partial \dot{u}}{\partial t}$$

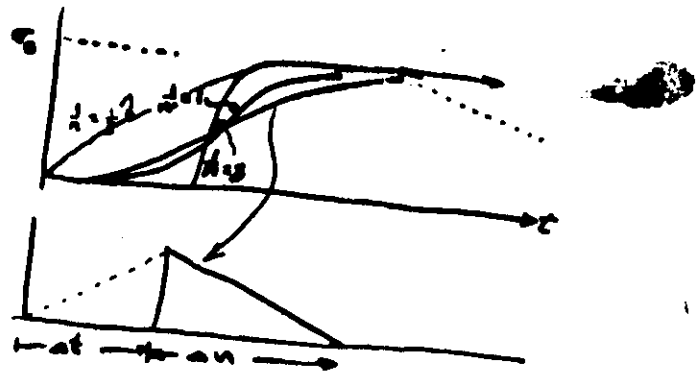

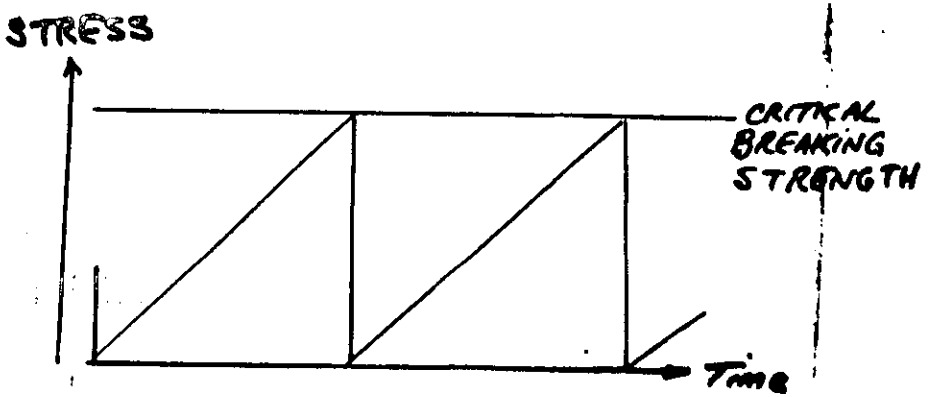

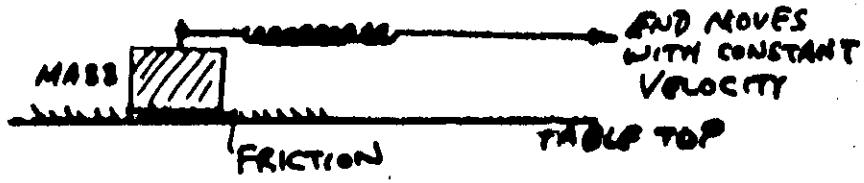

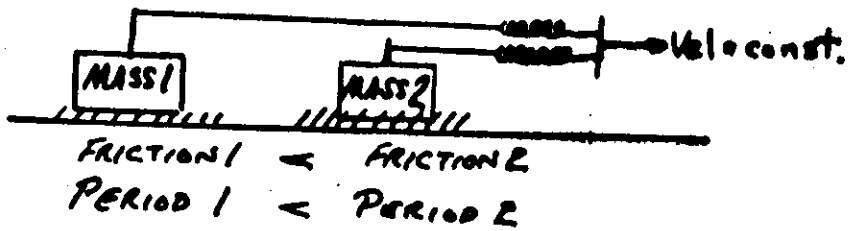

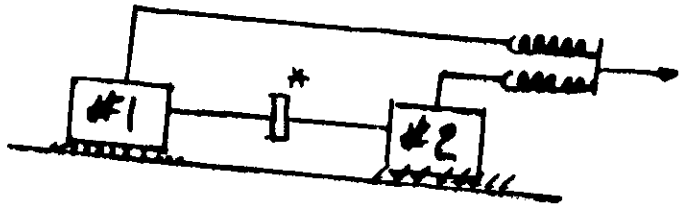

TRANSMITS FORCE WITH TIME DELAY

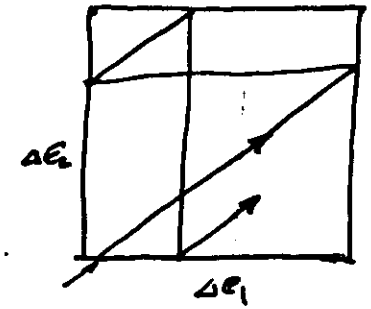

no coupling

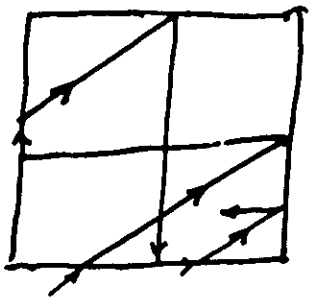

instantaneous coupling

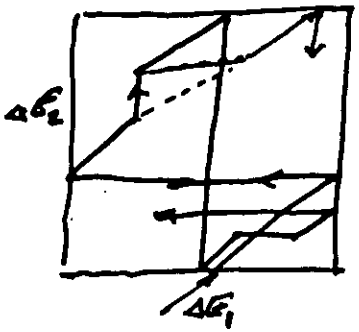

time-delay coupling (no decay) (decay)

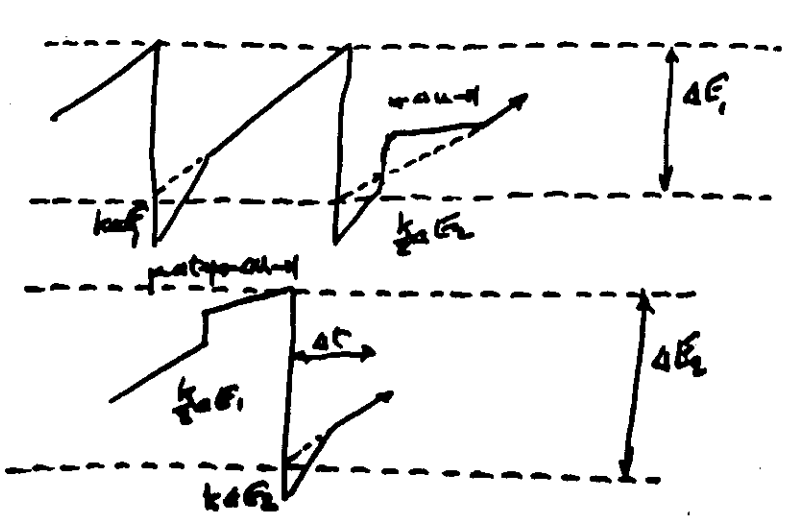

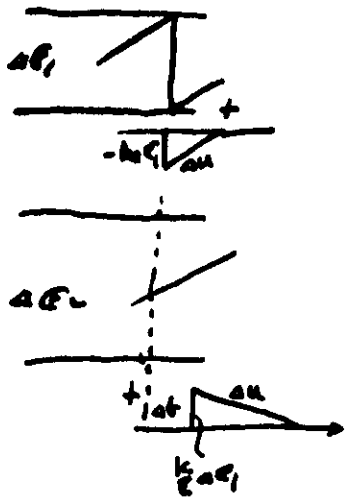

If $\Delta E_1 = \Delta E_2$
system is perfectly periodic

$\Delta E_1 \neq \Delta E_2$

Example:

$\Delta E_1 = \sqrt{.82}$ uncoupled $= \Delta T_1$

$\Delta E_2 = 1$ $= \Delta T_2$

k=4
k=8
k=3
k=7
k=2
k=6
k=1
k=5
Tw
z

Δt 0.25
k = 0.8
Δt = 0.15
Δu = 0.3
ΔTi = 0.05
ΔTc = 1
Δu=0.25
0.4
0.45
0.5
0.6
0.35
0.8
0.85
0.9
0.95
2.0
1.0

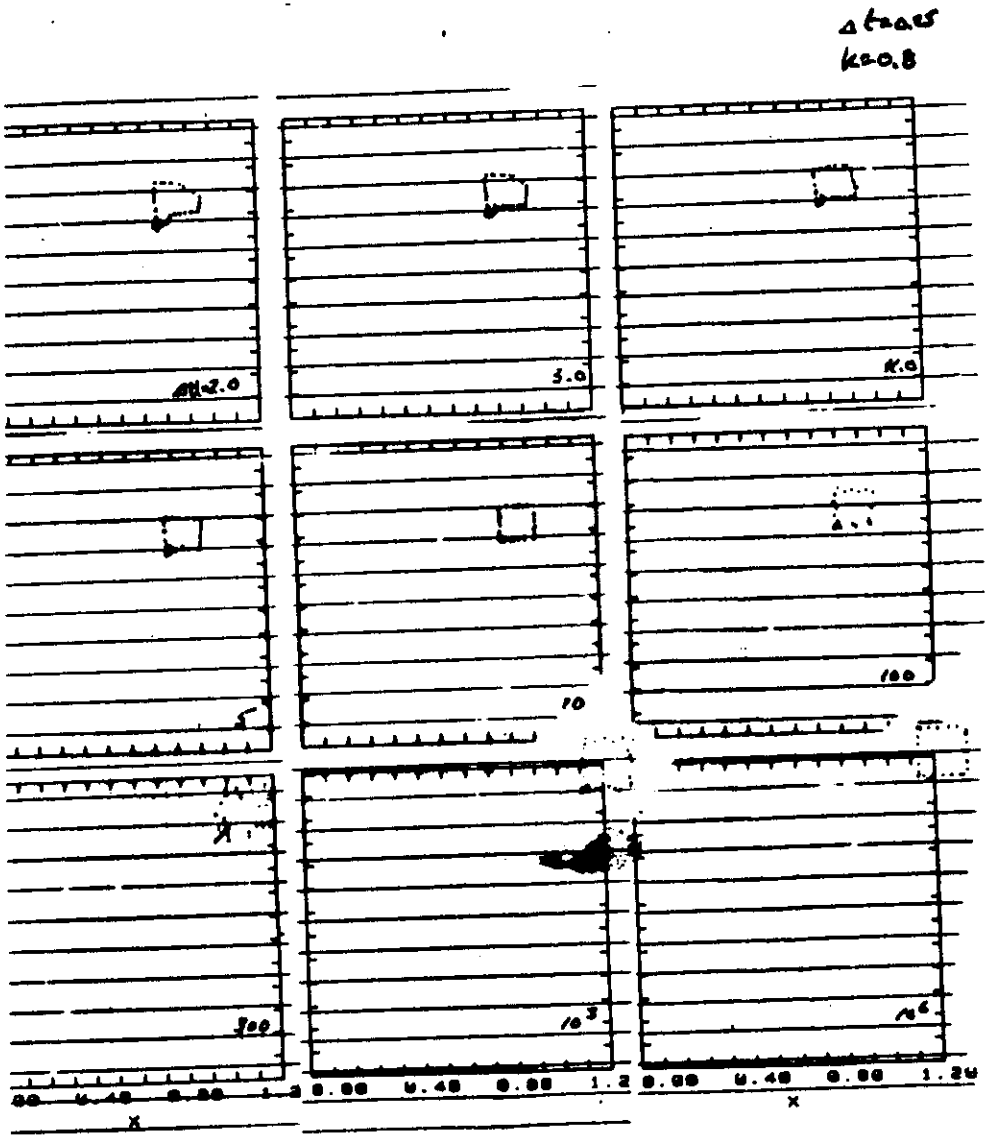

$n\Delta T_1$: n =		$n\Delta T_2$
0.905538514		0.961077028
0.905538514		0.905538514
0.905538514		0.905538514
0.905538514		1.322307431
0.905538514		1.000000000
0.716768917		1.000000000
1.000000000		1.000000000
0.999846624		1.000000000
0.905538514		1.000000000
0.905538514	11	0.922000680
0.905538514		0.905538514
0.905538514		0.905538514
0.905538514		0.905538514
0.905538514		1.361383779
0.905538514		1.000000000
0.905538514		1.000000000
0.755845265		1.000000000
1.000000000		1.000000000
0.960770276		0.977385818
0.905538514		0.905538514
0.905538514	10	0.905538514
0.905538514		0.905538514
0.905538514		1.305990641
0.905538514		1.000000000
0.905538514		1.000000000
0.905538514		1.000000000
0.700460127		1.000000000
1.000000000		1.000000000
1.000000000		0.938309470
0.921693928		0.905538514
0.905538514		0.905538514
0.905538514	11	0.905538514
0.905538514		1.343074989
0.905538514		1.000000000
0.905538514		1.000000000
0.905538514		1.000000000
0.905538514		1.000000000
0.739536475		0.993694608
1.000000000		0.905538514
1.000000000		0.905538514
0.977079066		0.905538514
0.905538514		1.289689851
0.905538514		1.000000000
0.905538514	10	1.000000000
0.905538514		1.000000000
0.905538514		1.000000000
0.905538514		1.000000000
0.905538514		0.954618260
0.684151337		0.905538514
1.000000000		0.905538514
1.000000000		0.905538514
0.938002718		1.328766199
0.905538514		1.000000000
0.905538514		1.000000000
0.905538514	11	1.000000000
0.905538514		1.000000000
0.905538514		
0.905538514		

$\Delta T_1 = 0.905538514 = 0.82^{1/2}$

$\Delta T_2 = 1.0$

$\Delta t = .15$ $k = 0.7$

$\Delta u = .3$

Reprint Series
19 June 1987, Volume 236, pp. 1563–1567

SCIENCE

Statistical Short-Term Earthquake Prediction

Y. Y. KAGAN AND L. KNOPOFF

Statistical Short-Term Earthquake Prediction

Y. Y. KAGAN AND L. KNOPOFF

A statistical procedure, derived from a theoretical model of fracture growth, is used to identify a foreshock sequence while it is in progress. As a predictor, the procedure reduces the average uncertainty in the rate of occurrence for a future strong earthquake by a factor of more than 1000 when compared with the Poisson rate of occurrence. About one-third of all main shocks with local magnitude greater than or equal to 4.0 in central California can be predicted in this way, starting from a 7-year database that has a lower magnitude cutoff of 1.5. The time scale of such predictions is of the order of a few hours to a few days for foreshocks in the magnitude range from 2.0 to 5.0.

AS FAR AS WE KNOW, THE ONLY practical approach to short-term earthquake forecasting that makes use of seismological data is one that uses foreshock activity to identify a larger, ensuing event. Typically, most investigators identify foreshocks long after the major event that follows them. After most large earthquakes have occurred, it is usually easy to identify precursory foreshocks. Although it is difficult to identify a seismological precursor while it is in progress, Jones (*1*) found there is a strong probability that smaller shocks are frequently followed by stronger events within a short time interval. In this report we apply a well-defined stochastic model for the probability that one earthquake will be followed by another of any size to the problem of the prediction of the likelihood of occurrence of a stronger shock. The model, which has only three adjustable parameters, has been derived from an independent, albeit significantly simplified, model of quasi-static fracture growth. A number of models of fracture give insights into the origins of certain features of seismicity, but, to our knowledge, this is the first time that the consequences of a theoretical model of fracture have been directly coupled to seismic data to derive a quantitative, nonempirical forecasting procedure.

We define a "prediction" to be a formal rule whereby the available space–time–seismic moment manifold of earthquake occurrence is significantly contracted and for which the probability of occurrence of an earthquake is anticipated to be significantly increased. We make no specification of the size of the second event of the pair here, except to require it to be stronger than the first.

The statistical reliability of most forecasts of the size, date, and place of a future individual earthquake is difficult to measure quantitatively. Strictly speaking, a forecasted earthquake that occurs just outside the prespecified time, space, and magnitude limits should be considered a failure, whereas, intuitively, the prediction was almost correct. Suppose that instead of the occurrence of one predicted strong earthquake, a cluster of slightly smaller, closely related earthquakes occurs that releases about as much energy. Has the prediction failed because the peak accelerations that were expected did not occur, or has it been successful because the total energy released is nearly equal to the predicted value? To respond to these questions we have developed a quantitative measure of the effectiveness or reliability of such predictions. As far as we know, no such measure has been proposed thus far, at least in the multidimensional case of interest to us.

At the present time the reliability of proposed prediction techniques is low. The occurrence of one false alarm (prediction of an earthquake that did not occur) does not disprove the validity of the arguments used in a prediction. If such predictions were formulated as a formal rule and applied to many earthquakes, it might be possible that the rule would actually "predict," that is, perform better than a Poisson random guess. Conversely, a single "successful prediction" does not validate a predictive procedure: an earthquake may occur just by chance, and we cannot tell whether the prediction was successful on its own merits or succeeded by coincidence.

We are concerned with the statistical prediction of strong earthquakes on time scales that are short (on the order of a few hours to a few days) when compared with the recurrence times of the strongest earthquakes, or with the prediction of aftershocks on time scales that are short when compared with aftershock inter-event times. Thus we avoid problems with the instability and variability of long-term earthquake sequences (*2*, *3*). Over short time scales, the dominant feature of statistical earthquake occurrence is a strong clustering of events in time and space (*2*–*4*).

Quantitative prediction requires that we estimate future occurrence rates on the basis of probability at all points of the space–time–seismic moment manifold for any possible earthquake sequence. To do this we define a continuous function that is derived from a stochastic model and is parametrically fitted to the available history of seismicity. We then extrapolate the fitted function to perform the prediction; the effectiveness of the prediction and its accuracy can be evaluated quantitatively. The seismic histories are contained in one of the catalogs of earthquake occurrence (*5*). These catalogs list earthquakes and give their origin times, their locations in three dimensions, and occasionally focal mechanisms in the form of either fault-plane or seismic moment tensor solutions or both.

We have introduced two quantities that are related to the prediction problem (*6*). The first is the predictive ratio $\Lambda(t, \mathbf{x}, M)/\Lambda_0(\mathbf{x}, M)$, where $\Lambda(t, \mathbf{x}, M)\Delta t$ is the probability that an earthquake occurs at time t during a small time interval Δt, at location (and possibly focal parameters) $\mathbf{x}$, and with scalar seismic moment M. The conditional probability $\Lambda\Delta t$ is computed for some model to be tested (*2*) for a given history of seismicity. The quantity $\Lambda_0(\mathbf{x}, M)\Delta t$ is the same probability according to the Poisson hypothesis. The predictive ratio (or its maximum value) has been adopted by some investigators to characterize the effectiveness of a forecast (*7*, *8*).

The second quantity is the information content (I), which is the base 2 logarithm of the integral of the predictive ratio over the space–time–seismic moment manifold (*4*, *6*, *9*). This quantity can be written as the sum of two terms,

$$I = -\log_2 e \int_0^T \int_{\mathbf{X}} \int_{M_c} [\Lambda(t, \mathbf{x}, M \mid \boldsymbol{\chi}) - \Lambda_0(\mathbf{x}, M \mid \boldsymbol{\chi}_0)]\, dt\, d\mathbf{x}\, dM + \int_0^T \int_{\mathbf{X}} \int_{M_c} \log_2 \frac{\Lambda(t, \mathbf{x}, M \mid \boldsymbol{\chi})}{\Lambda_0(\mathbf{x}, M \mid \boldsymbol{\chi}_0)}\, dN(t, \mathbf{x}, M) = (\ell - \ell_0)/\ln 2 \quad (1)$$

where the $\boldsymbol{\chi}$ values are the parameters of the model; T and $\mathbf{X}$ are, respectively, the time and space spans of the catalog; M_c is the seismic moment cutoff of the catalog; $dN(t, \mathbf{x}, M)$ are multidimensional delta functions corresponding to the earthquakes in the catalog; ℓ is the logarithm of the likelihood for the particular model of earthquake occurrence; and ℓ_0 is the logarithm of the likelihood for the Poisson model. Because the Poisson process has maximum entropy for a given rate of occurrence, it is an ideal reference model for measuring the information content of any competing model. Frequently a single catalog entry spans a large

Institute of Geophysics and Planetary Physics, University of California, Los Angeles, CA 90024.

number of subevents that have occurred between the beginning of rupture and the next event in the catalog. Thus the total time span in Eq. 1 includes a "dead time" after each earthquake in the catalog. We systematize these dead times against inconsistencies in identifying aftershocks by taking the dead time to be the coda time computed according to Eq. 4. These dead times can be considered to be one version of a weighting function that suppresses very short time influences. Other rules for incorporating weighting functions are possible.

The values of the parameters χ in Eq. 1 are chosen to maximize the logarithm of the likelihood function $\ell = \ell_0$. These parameters are selected in view of certain assumptions regarding the stresses at the edge of an earthquake fracture (*10*). Depending on the details of the particular model and the assumptions, the number of parameters in our models is between three and seven.

We assume that the clusters of foreshocks and aftershocks have a Poisson distribution, although the individual events within the cluster do not. The conditional density or hazard function $\Lambda(t, \mathbf{x}, M)$ is (*11–13*)

$$\Lambda(t, \mathbf{x}, M) = \lambda \cdot \phi(\mathbf{x}, M) + \sum_i \psi_{M_i}(t - t_i, \mathbf{x} - \mathbf{x}_i, M) \quad (2)$$

where λ is the rate per unit time of Poisson occurrence of a cluster, the first shock of which has seismic moment greater than or equal to M in the volume $(\mathbf{X})$; $\phi(\mathbf{x}, M)$ is their space–seismic moment distribution; $\psi_M(t - t_i, \mathbf{x} - \mathbf{x}_i, M)$ is the conditional distribution of later events occurring at time t and coordinates $\mathbf{x}$, if earlier earthquakes have occurred at times t_i and coordinates $\mathbf{x}_i$. For the purposes of the illustration below, we shall assume that an "alarm" is declared when the hazard function exceeds a certain "threshold" rate.

The conditional distribution of the jth shock, which depends on the occurrence of the ith independent shock ($j > i$) with seismic moment M_i, is

$$\psi_{M_i}(\tau_{ij}, \rho, \zeta, M_j) = \nu(M_j) \cdot \psi_t(\tau_{ij}) \cdot \psi_\rho(\rho) \cdot \psi_\zeta(\zeta) \cdot \phi_M(M_j) \quad (3)$$

where $\tau_{ij} = t_j - t_i$ ($\tau > 0$); ρ is the horizontal distance between the ith and jth epicenters; $\zeta = z_j - z_i$ is the vertical distance between the hypocenters; $\nu(M_j)$ is the total number of dependent shocks "generated" by a shock with seismic moment M_i; $\psi_*(*_{ij})$ are conditional density distribution functions (the asterisk indicates the three possible arguments of the functions); and $\phi_M(M_j)$ is the unconditional distribution density function of the seismic moment (*14*).

We have estimated the values of the parameters of the model of Eq. 2 and the information content for the part (1971 through 1977) of the California Network (CALNET) (U.S. Geological Survey) catalog for central California (*15*) that is in final form (*16*); more recent catalogs have not been winnowed to eliminate spurious events. The magnitude threshold for the catalog has been taken to be 1.5 (*4, 15*). There are 7360 events in the catalog.

The occurrence of one earthquake raises the probability level immediately; it then decays rapidly at a rate that depends on the scalar seismic moment M of the earthquake and the time that has elapsed since the earthquake's occurrence τ (*2, 3*):

$$\psi_M(\tau) = \nu(M) \cdot \psi_t(\tau) = \frac{\mu}{2}\left[\frac{M}{M_c}\right]^{2/3}\left[\frac{t_M}{\tau^3}\right]^{1/2} \text{ for } \tau \geq t_M \quad (4)$$

where the total number of dependent events is $\mu(M/M_c)^{2/3}$ and t_M is the time span of the coda waves of an earthquake with seismic moment M. The values of t_M and M_c depend on the properties of the seismographic network. For the CALNET catalog we take t_M to be 3.46×10^{-3} day for an earthquake with scalar seismic moment $\log_{10} M = 22.4$ [local magnitude (m_L) about 4.0] (*17*) and $\log_{10} M_c = 18.6$ (m_L about 1.5). The coda duration t_M is proportional to the cube root of the seismic moment (*3*). We set $\mu = 0.075$. Numerical tests show that the results of the predictions are not influenced significantly by changes in the value of μ. A change of μ is simply equivalent to a change of the alarm threshold rate for large values of the alarm threshold rate; the value of μ influences the prediction efficiency only for values of the threshold rate close to the Poisson rate.

Introduction of the epicentral coordinates into the fitting process (Eq. 3) increases the information content by a factor of from 5 to 10. The use of depth data in Eq. 3 increases the information content by only about 15%; this effect is small because of the high redundancy in the narrow depth range of the hypocenters in the CALNET catalog. To illustrate the use of Eq. 3, we neglect all of the conditional distributions other than those for origin times and one-dimensional locations of a projection of the epicenters on the trace of the San Andreas fault, which we take to be approximately N37°W in this region. In Table 1, the values of I and ℓ are calculated for subcatalogs consisting of 1-year intervals and five equal 73-km portions of the San Andreas fault zone, with the first segment being the northernmost.

Although these quantities fluctuate strongly over the temporal and spatial subdivisions of the catalog, closer inspection shows that the value of I depends strongly on the occurrence of large clusters of earthquakes; most often, but not necessarily, these clusters are the aftershocks of some strong event. An indicator of the presence of a large aftershock sequence is the appearance of a large value of the maximum magnitude m_{max} in the catalog.

We estimate the probability of occurrence of future earthquakes from Eq. 2. The adjustable parameters χ are given by a maximum likelihood procedure. Some of the parameters are obtained from other physical or geological considerations (*3, 10, 14*); both the unconditional and conditional predicted distributions of earthquake sizes (Eq. 3) are assumed to obey the Gutenberg-Richter law or its modification for the distribution of the seismic moment tensor (*14*). As a direct consequence of the latter assumption, we make no attempt here to "predict" the seismic moment or any other measure of the size of a future earthquake. Only the time–multidimensional space probability or seismic activity has been extrapolated from the available data.

Figure 1 shows an example of the hazard function, or the prediction, as a function of time. We take the spatial distribution to be Gaussian

$$\psi_\xi(\xi) = (\sigma\sqrt{2\pi})^{-1} \cdot \exp[-\xi^2/(2\sigma^2)] \quad (5)$$

where ξ is the distance between shocks along the line. The value of σ is estimated to be about 0.5 km for an earthquake with $\log_{10} M = 22.4$ ($m_L = 4.0$); σ is proportional to the cube root of the scalar seismic moment.

The hazard function displayed in Fig. 1A spans the interval from 22 to 29 February 1972 for one point on the San Andreas fault in Bear Valley, California (*18*), a time of particularly vigorous activity. Most of the time-location space is significantly less densely studded with alarms. The number of independent events in the full catalog is estimated to be 5355. The reference Poisson rate is 0.0058 earthquake/(day times kilometers), which we assume to be a constant for the entire fault and the entire period of the catalog. For purposes of illustration, we chose the threshold rate for an alarm to be ten times the Poisson rate.

The spikes are the functions $t^{-3/2}$. The peaks of the functions for the stronger events are not as large as those for the smaller events, since the conditional rate function is plotted only from the end of the coda, and larger earthquakes have larger coda times. However, the influence of stronger shocks can be recognized on the display by longer decay times. Figure 1B shows those earthquakes in this time period whose epicentral projections are close to the "prediction" point. The reduced influence of more remote earthquakes can be discerned.

The display is characterized by two significant alarm bursts above threshold. The strongest earthquake ($m_L = 3.5$) in the first burst occurred about 0.5 day after the alarm had been declared at about 0.2 day. The largest event ($m_L = 4.6$) occurred shortly after the second alarm at about 6 days. Two of the three small earthquakes that immediately preceded the largest event triggered separate alarms, but in each case the shocks were so small that the probability function fell rapidly below threshold. Considered rigorously, all of the shocks above the threshold in Fig. 1 were forecast successfully except those that "turned on" alarms; however, most of the shocks must be considered aftershocks, for which we cannot take much credit. A first "predicted" earthquake starts an alarm and "predicts" a second, even stronger earthquake; if no second event occurs that is stronger during the prolongation of the burst, we have generated a false alarm. Thus, every burst must be a generator of one false alarm, even if it contains one or more successful predictions. Similarly, the declaring of an alarm is by definition a failure-to-predict, and every burst is identified with one such failure.

Some of these relations become clearer if we consider the space-time hazard function. Figure 2 shows the locations and times that are above the threshold for a 10-km segment of the San Andreas fault in the Bear Valley area for the same time interval as in Fig. 1. The disconnected alarms of Fig. 1 near $t = 6$ days are in reality connected; the disjoint nature of the alarm intervals in Fig. 1 arose because of our failure to display spatial variations. Figure 1 represents a section through Fig. 2 at a coordinate that cuts across the decays for the first two events. The complexity of the interconnections is associated with the complexity of the geometry of earthquake occurrence, which has been shown to have a fractal character (*2, 19*). The complexity of the blotchy pattern will probably increase as the number of dimensions of the prediction space increases.

The ratio of the total size of all alarm zones to the total space-time size of the catalog is shown in Fig. 3 as a function of the threshold level. As may have been expected, the space-time areas of the alarm zones decrease as the prediction threshold is raised. Also displayed is the ratio of the number of events that fall into the alarm zones to the total number of earthquakes in a given catalog. The latter ratios have been calculated (i) for main earthquakes with $m_L = 3.5$ or greater that have been preceded by foreshocks, that is, by smaller earthquakes that triggered the alarm; and (ii) for all events with $m_L \geq 1.5$; in this case, we count aftershocks as well as main shocks as "successes."

For a threshold ratio of 10^3, for example, the total size of the dangerous zones is 9×10^{-3} of the total time-distance area; 7.1% of all earthquakes with $m_L \geq 1.5$, 6.6% of 301 main shocks with $m_L \geq 3.0$, 10% of 58 main shocks with $m_L \geq 3.5$, and 14% of 21 main shocks with $m_L \geq 4.0$ occur in these zones. For low levels of the threshold ratio, the maximum percentage of successes, that is, the number of earthquakes with $m_L \geq 4.0$ that are preceded by foreshocks, is about 33%. If we take the threshold to be equal to the Poisson rate and assume that shocks occur uniformly over the entire fault, almost all of the earthquakes

Table 1. Likelihood function for the CALNET catalog of earthquakes and its time and space subdivisions. Abbreviations: n, number of events; m_{max}, maximum magnitude; ℓ, logarithm of the likelihood; I/n, information content ratio.

Time or space interval	n	m_{max}	ℓ	I/n
Time intervals, all space				
1971	784	3.9	773.0	1.42
1972	1511	5.0	2760.2	2.64
1973	1013	4.6	912.7	1.30
1974	946	5.2	876.6	1.34
1975	1004	4.9	583.8	0.84
1976	1061	4.3	791.3	1.08
1977	1041	4.3	1239.4	1.72
Space intervals, all time				
1	96	3.2	45.6	0.69
2	736	4.3	1370.6	2.69
3	1750	5.2	1210.2	1.00
4	3719	5.0	4211.9	1.63
5	1059	4.9	401.9	0.55
All space-time intervals				
	7360	5.2	8080.2	1.58

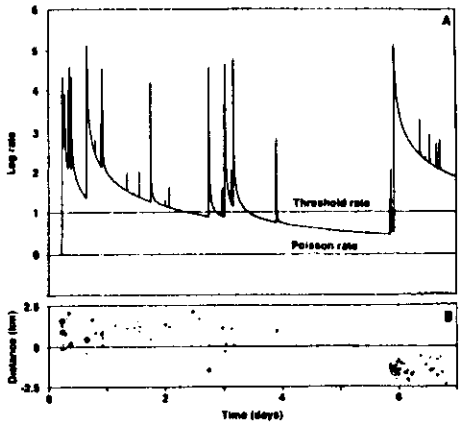

Fig. 1. (**A**) Conditional rate of occurrence of earthquakes or hazard function for Bear Valley, California, $t = 0$ is 22 February 1972, 0000 Greenwich Mean Time. The threshold rate is ten times the Poisson rate. (**B**) A time-distance plot of earthquake occurrence; the sizes of the symbols are roughly proportional to the magnitudes of the events. The center line, marked at 0, in (**B**) corresponds to the reference point of the diagram in (**A**).

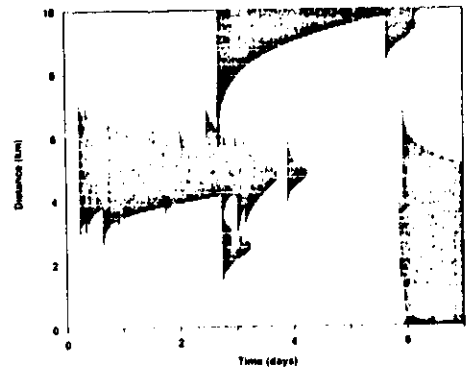

Fig. 2. Earthquake hazard map for a 10-km segment of the San Andreas fault in Bear Valley, California. The time scale is the same as in Fig. 1. The reference point for Fig. 1 is at coordinate 4 km. The shaded areas indicate predicted rates that exceed the threshold rate. The threshold rate is ten times the Poisson rate.

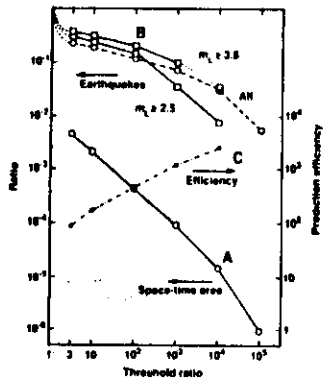

Fig. 3. Prediction efficiency for a 7-year, 364-km interval of the San Andreas fault in central California. Threshold rates are in units of the Poisson rate. Curve A, ratio of the total space-time size of all dangerous zones to the total space-time size of the catalog. Curves B, ratio of the number of events falling into dangerous zones to the total number of earthquakes. The dashed line represents main shocks and aftershocks for all events with $m_L \geq 1.5$. Curve C, prediction efficiency for main shocks with $m_L \geq 3.5$.

will be predicted, since almost all of the space-time span of the catalog will be an alarm zone; the value of this "prediction" is nil.

Similarly, the occurrence of a single very large earthquake raises the probability function to such a high level that an alarm, presumably for aftershocks, is declared that may endure for a number of years. Under the assumption that the triggering earthquake is the only one holding the alarm open, for a limited range of local magnitudes the number of days that an alarm will be open is $0.0154 \times 10^{0.5m_0} \times r_t^{-2/3}$, where r_t is the relative threshold rate, for distance $\xi = 0$ (Eq. 5). Most, if not all, of the strong aftershocks of any earthquake can be predicted by our procedure. Even though predictions of aftershocks do not have the same visibility as the prediction of main shocks, strong aftershocks can be dangerous, and they represent an area of significant engineering and public concern.

The ratio of the percentage of earthquakes predicted to the percentage size of the dangerous zones gives an estimate of the improvement in the prediction over the Poisson assumption. We call this ratio the efficiency of the prediction. For earthquakes with $m_L \geq 3.5$ the efficiency is about 1100 for a threshold ratio of 10^3 (Fig. 3). We prefer to use the efficiency instead of the false alarm rate as a measure of success or failure of the prediction; our representation always predicts false alarms. The efficiency of prediction of future main shocks increases with increase in the magnitude of the main shock.

The drop in the success rate with increasing threshold ratio is small up to a ratio of about 10^2; hence, up to this threshold, the space-time size of the alarm zones can be reduced strongly without major reduction in the success rate. Beyond this threshold the success rate falls off rapidly, at least for this earthquake catalog. The difference between the success rate and 100% is the rate of failures-to-predict; as the threshold level increases, both the efficiency of the prediction and the rate of failures-to-predict increase (Fig. 3).

Criteria for alarm onset and call-off may have to be modified according to the user's needs. Such modifications could result in different failure-to-predict rates than those reported here. The choice of the appropriate weighting function (Eq. 1) and the threshold level are discretionary parameters for the users of the prediction technique.

Figure 2 displays the space-time zones of increased probability of occurrence of earthquake epicenters. To predict the damage caused by larger earthquakes, we will have to take into account the size of the rupture zone, as well as other engineering features such as propagation effects, soil conditions, and attenuation; these aspects of the problem are not considered here.

We estimate the maximum effectiveness of our procedures by calculating the specific information content per event, I/n, in a model that simulates the complete process. The output of a stochastic model of earthquake occurrence that simulates the Poisson cluster process well (*2, 3, 19*), with parameters appropriate to the CALNET catalog, yields from 10 to 15 bits of information per earthquake, if the synthetic catalog is processed in the same way as above. We believe the major reason for the difference is that although our synthetic catalogs include large earthquakes, there are no large earthquakes in the period 1971 through 1977 for the CALNET catalog; the largest earthquake ($m_L = 5.2$) ruptured only about 3% of the total length of the fault. Support for this interpretation is found by noting that during the prominent Bear Valley sequence of earthquakes of 1972 (*18*) the value of I/n was significantly larger than during all of the other years of the catalog (Table 1). Comparison with other earthquake catalogs shows that an increase in the length of the catalog does not necessarily reflect an increase in the bit rate per earthquake; the latter quantity depends on the quality of the seismographic network and on the presence of large earthquakes in the catalog (*4*).

Because the ratio of I/n for the theoretical result is larger than that derived from the observations, it might be possible that the uncertainty in earthquake occurrence can in principle be reduced by a factor of 2^{10} when compared with the Poisson model, since each bit of information reduces the uncertainty by a factor of 2. These estimates are somewhat suspect because we do not know the numbers of degrees of freedom either in the stochastic model or in the result of processing by Eq. 1. We cannot assess the influence of inadequacies due to the use of the branching process simulation model in the stochastic model, nor can we assess the influences of misidentification, origin time and location errors, the selection of arbitrary thresholds, and the use of models such as the magnitude-frequency law, in the analysis of actual data. However, we know that the absence of large earthquakes in the test period gives a significantly low value of the specific information content. Although both foreshock–main shock and main shock–aftershock sequences are used in the computation of the information content, most of the information is supplied by the latter sequences, which are of less interest for purposes of prediction. However, the results of statistical analysis of earthquake catalogs (*3, 4*) and those of the modeling of the occurrence of earthquakes by a self-similar stochastic model (*2, 19*) indicate that both foreshocks and aftershocks are manifestations of essentially the same process, namely, the stochastic interaction of earthquakes. We interpret our model as an indication that we are able to derive the likelihood of the triggering of one earthquake by another but that we do not know whether the succeeding earthquake will be larger than the preceding one; the next level of refinement of this model will involve computation of the relative magnitudes of the events.

In view of these comments it is startling that the estimates of the effectiveness of predictions based on the information content are of the same order of magnitude as those obtained from the hazard function (Fig. 3). This agreement may be coincidental because the methods may have different numbers of degrees of freedom and constraints. The information content is suited for theoretical studies of earthquake occurrence, whereas the hazard function is more useful for earthquake forecasting. The information content for the CALNET catalog decreases rapidly if the dead time is increased beyond the coda time. After 1 hour, 10% of the predictive information is lost; 1 day later, the reduction is one-third; and 10 days later it is one-half (*3*). In addition, the failure-to-predict rate increases rapidly with increasing dead time. The information content for the best seismological data presently available is not an upper limit. But it may be increased significantly through the introduction of seismic moment tensor information and estimates of stress from geological and geodetical investigations as well as from past earthquakes.

Our results indicate that only about one-third of the strong earthquakes are preceded by foreshocks that are separated in time from an independent shock by more than t_M. For other modern catalogs of earthquakes that are similar in quality to the central California CALNET catalog, the number of failures-to-predict is about the same, that is, of the order of two-thirds (*1, 3, 4*).

A modification of the above strategy for prediction is called for in the case of the occurrence of strong earthquakes. Strong earthquakes have the potential for serving as foreshocks of even stronger earthquakes, or they may be the main shock in the sequence, just as weaker earthquakes can serve both functions. However, the coda time t_M is about 15 minutes for an earthquake with $m_L = 5$, and this time increases by a factor of about $\sqrt{10}$ for a unit increase in earthquake magnitude. If an earthquake with $m_L = 6$ were to occur, with or without prior warning according to the scenario above, no alarm for a possibly even stronger earthquake would be sounded for about $t_M = 50$ minutes, which might be an unacceptably long delay for issuing a warning. This difficulty is circumvented if we reduce the dead time for large earthquakes to a value less than the coda time.

This modification for strong earthquakes indicates that response strategies can also be developed with time delays of the order of seconds. As suggested by Heaton (*20*), it may be possible to predict some large earthquakes through the analysis of small starting phases of complex events that later blossom into large earthquakes. These small starting phases are genuine earthquakes whose signals overlap with those of their successors and raise the probability level for a short time, thereby triggering an alarm for the larger event. The number of these preshocks should increase as $t_b^{-1/2}$, where t_b is the time before the start of the main phase of a strong earthquake (*2–4*). In the present method, we are not restricted to dead times of the order of rupture times, but instead we are able to use longer delays of the order of a few minutes. With this procedure there should be far fewer failures-to-predict for very strong earthquakes. Automated response strategies could take advantage of these predictions in a well-developed technology.

The differences between our proposed forecasting technique and methods that use empirically derived probabilities of foreshock–main shock occurrence may be summarized as follows. (i) Since our model is based on a formulation derived from a multidimensional stochastic process, it is not necessary to use arbitrary windows to analyze seismicity nor is it necessary to delete aftershocks from a catalog to make the catalog amenable to statistical analysis. Therefore, our forecasts are not dependent on a post-factum classification of earthquakes into fore-, main, and aftershocks, a subdivision that may not be possible in real time. (ii) Since the parameters of our seismicity model are obtained through a maximum likelihood procedure, the model is optimal in a quantitative way. The choices of the parameters can be justified on the basis of a well-defined theoretical model of earthquake occurrence (*2, 10, 19*). Furthermore, the model itself is consistent with all of the other aspects of statistical seismicity that have been well documented, and it has not been derived for the sole purpose of developing the foreshock–main shock relations. The model has only three parameters that are adjusted to the properties of the local seismicity: the rate of occurrence of independent earthquakes and the coefficients that specify the occurrence of dependent earthquakes, μ and σ. In one sense the exponent 2/3 in Eq. 4 is also an adjustable parameter, but since this can be derived on formal grounds (*3*), we have considered it as fixed. (iii) The likelihood function we have derived allows us to estimate the effectiveness of the proposed prediction scheme in terms of information content of an earthquake catalog. The procedures outlined here can be adapted to predicting schemes other than the one we have used, as soon as the quality and quantity of the data describing these precursors reach the stage where they can be processed by similar multidimensional statistical techniques.

REFERENCES AND NOTES

1. L. M. Jones, *Bull. Seismol. Soc. Am.* **75**, 1669 (1985).
2. Y. Y. Kagan and L. Knopoff, *J. Geophys. Res.* **86**, 2853 (1981).
3. ———, in preparation.
4. ———, *Geophys. J. R. Astron. Soc.* **55**, 67 (1978).
5. W. Rinehart, H. Meyers, C. A. von Hake, *Summary of Earthquake Data Base* (National Geophysical Data Center, Boulder, CO, 1985).
6. Y. Kagan and L. Knopoff, *Phys. Earth Planet. Inter.* **14**, 97 (1977).
7. D. Vere-Jones, *J. Phys. Earth* **26**, 129 (1978).
8. K. Aki, in *Earthquake Prediction, An International Review*, D. W. Simpson and P. G. Richards, Eds. (Maurice Ewing Series, no. 4, American Geophysical Union, Washington, DC, 1981), p. 566.
9. E. Papageorgiou, *Z. Wahrscheinlichkeitstheorie verw. Geb.* **44**, 191 (1978).
10. Y. Y. Kagan and L. Knopoff, *Geophys. J. R. Astron. Soc.* **88**, 723 (1987).
11. I. Rubin, *IEEE Trans. Inf. Theory* **IT-18**, 547 (1972).
12. T. Ozaki, *Ann. Inst. Stat. Math.* **B31**, 145 (1979).
13. D. Vere-Jones and T. Ozaki, *ibid.* **B34**, 189 (1982).
14. Y. Y. Kagan and L. Knopoff, *Proc. 8th Int. Conf. Earth. Eng.* **1**, 295 (1984).
15. S. M. Marks and F. W. Lester, *U.S. Geol. Surv. Open-File Rep.* **80-1264** (1980), and references therein.
16. See (4), p. 69.
17. W. H. K. Lee *et al.*, *U.S. Geol. Surv. Open File Rep.* (1972).
18. W. L. Ellsworth, *Bull. Seismol. Soc. Am.* **68**, 483 (1975).
19. Y. Y. Kagan, *Geophys. J. R. Astron. Soc.* **71**, 659 (1982).
20. T. H. Heaton, *Science* **228**, 987 (1985).

21. Supported in part by grant CEE 84-07553 from the National Science Foundation. We acknowledge useful discussions with G. M. Mokhtan. Publication 2962, Institute of Geophysics and Planetary Physics, University of California, Los Angeles, CA 90024.

4 August 1986; accepted 1 April 1987

JOURNAL OF GEOPHYSICAL RESEARCH, VOL. 86, NO. B4, PAGES 2853-2862, APRIL 10, 1981

STOCHASTIC SYNTHESIS OF EARTHQUAKE CATALOGS

Y. Y. Kagan and L. Knopoff

Department of Physics and Institute of Geophysics and Planetary Physics
University of California, Los Angeles, California, 90024

Abstract. A model of earthquake occurrence is proposed that is based on results of statistical studies of earthquake catalogs. We assume that each earthquake generates additional shocks with a probability that depends on time as $t^{-(1+\theta)}$. This assumption together with one regarding the independence of branching events on adjacent branches of the event 'tree,' is sufficient to permit the generation of complete catalogs of earthquakes that have the same time-magnitude statistical properties as real earthquake catalogs. If θ is about 0.5, the process generates sequences that have statistical properties similar to those for shallow earthquakes: many well-known relations are reproduced including the magnitude-frequency law, Omori's law of the rate of aftershock and foreshock occurrence, the duration of a recorded seismic event versus its magnitude, the self-similarity or lack of scale of rate of earthquake occurrence in different magnitude ranges, etc. A value of θ closer to 0.8 or 0.9 seems to simulate the statistical properties of the occurrence of intermediate and deep shocks. A formula for seismic risk prediction is proposed, and the implications of the model for risk evaluation are outlined. The possibilities of the determination of long-term risk from real or synthetic catalogs that have the property of self-similarity are dim.

1. Introduction

Most theoretical solutions to problems in fracture dynamics yield relatively simple source-time functions: the velocity of slip functions generally rise monotonically and then decrease monotonically until all motion eventually ceases. On the other hand, there is some circumstantial evidence that real earthquake source-time functions are not simple functions of time; the velocity of slip functions may be rather more serrated, which would indicate that if the motion due to a single event is simple, the source must be a superposition of a number of rupture events. In this paper, we make this postulate and derive source-time functions based on it.

We have noted elsewhere [Kagan and Knopoff, 1978, 1980b] that Omori's law of the rate of occurrence of aftershocks seems to be a universal phenomenon. This law, which is that the rate of occurrence of aftershocks varies as $1/t$, has been verified for catalogs of the largest earthquakes on a worldwide scale as well as for catalogs on smaller regional scales, at least when the available catalogs are reasonably well documented. Extended back to the origin time of an earthquake, the rate of occurrence literally approaches infinity. We shall make the assumption that this rate of occurrence relation holds even at such a short time scale that the interval between events is less than the duration of the relative faulting motions of an individual event.

In this paper we make several simplifying assumptions. First, we shall assume that the source is a point in space. Second, we assume that the individual shocks in a complex source event are discrete in such a way that each component event of the complex sequence contributes a waveform to the motion having the same time-dependence as all the others. Third, we assume that the source-time function is a simple step function of displacement; this may be wrong in detail, but it is sufficient for the purposes of simulating real catalogs, as will be seen below.

By virtue of the time scale independence of power law functions we may imagine that the source-time function of a single earthquake, composed of a superposition of overlapping individual events, is identical to that of the history of deformation of the earth due to repeated earthquakes over years or even centuries under a suitable change of time scale. The best statistical information we have today relates to earthquake occurrences over intervals of years. In this paper we assume that we can extend the known statistical properties of earthquake catalogs to the time scale of earthquake durations at the source. We use a model which employs a minimum number of parameters. We will show that this model provides an adequate source-time function that simulates well the statistics of individual earthquake events and simulates the relationships between earthquakes in real catalogs as well. We simulate individual earthquakes by a Monte Carlo procedure, obtain synthetic catalogs of earthquakes, investigate statistical properties of these catalogs, and compare the results with the corresponding properties of real earthquake catalogs.

2. Stochastic Self-Similarity of the Earthquake Process

Before embarking on a description of the properties of earthquake source-time motions synthesized according to models incorporating some of the ideas sketched above, we review some of our recent results relating to the stochastic interaction of earthquakes. The most important feature which emerges as a result of these investigations [Kagan and Knopoff, 1977, 1978, 1980a, b], is the stochastic self-similarity of the seismic process, i.e., the absence of any particular scale connected with time-distance-magnitude patterns of earthquake occurrence. This self-similarity manifests itself in the appearance of power law distributions of all the features of the earthquake process investigated thus far: the power law distribution of seismic energies or moments, Omori's power law for the rate of occurrence of aftershocks and foreshocks of shallow earthquakes, the power law distribution of the energies of foreshocks and aftershocks, and the inverse power law dependence of the spatial moment on the separation between two foci. Some generalizations of the ideas of stochastic self-similarity are presented by Mandelbrot [1977].

We have found [Kagan and Knopoff, 1978, 1980b] that self-similarity holds over a magnitude range extending from $M = 1.5$ to the greatest earthquakes. Because of the absence of dimensional scaling parameters we make the assumption that the rate of occurrence of foreshocks of small earthquakes and small aftershocks of small earthquakes is similar to that for large events with only the time and distance scales changed appropriately. In this paper, we only use the assumption with regard to the time scale.

The time-magnitude rate of occurrence of statistically dependent earthquakes is shown schematically in Figure 1. The upper figure shows the time rate of occurrence for a given magnitude difference between the events. It is symmetric for the case in which the magnitude difference between a foreshock and its succeeding larger event and a larger event and its succeeding smaller aftershock is virtually zero. The asymmetry of the time behavior of the seismic process, that is, that there are few if any foreshocks and an abundance of aftershocks, is explained by their different magnitude distributions (see lower part of Figure 1). The number of aftershocks increases as ΔM increases, whereas the number of foreshocks decreases with increasing ΔM.

As we have indicated, the large rate of occurrence of dependent events near the origin time of a main earthquake means that we assume that we can model each earthquake as a merger of many shocks [Kagan and Knopoff, 1978]. This multishock aspect of earthquake occurrence is illustrated schematically in Figure 2, where the

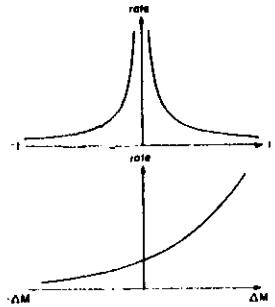

Fig. 1. Rate of occurrence of dependent shocks. The upper curve shows the rate of occurrence of foreshocks on the left and of aftershocks on the right for the case when these shocks are comparable in size to the main event ($\Delta M = 0$). The lower plot displays schematically the distribution density of dependent shocks versus magnitude difference ΔM. The lower curve therefore represents a multiplying factor to be applied to the upper curve for a given value of ΔM.

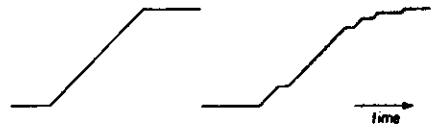

Fig. 2. Schematic illustration of seismic moment release in a multiple event (right) in comparison with the conventional picture.

single event in the left-hand portion of the diagram is replaced by several shocks whose origin times occur according to the statistical laws illustrated in Figure 1. There are some indications in real earthquakes for patterns of multishock occurrence [Trifunac and Hudson, 1973].

We assume that there is nesting of shocks: referring to Figure 2, perhaps each of the smaller steps in the right-hand part of the diagram should be replaced by an even smaller set of replicas of the whole process occurring on a shorter time scale. If our hypothesis is correct, then a real record shows a somewhat smoothed picture of the superposition of traces from many shocks having a dense distribution in time.

3. Stochastic Model of Earthquake Process

We describe a stochastic model of an earthquake process whose properties depend on only two significant intrinsic parameters. The model is designed to generate a simulated seismicity that is statistically equivalent to the time-magnitude properties of real earthquakes. Although there is no intrinsic size of earthquakes in our model, for convenience a unit earthquake with seismic moment m_0 is introduced on an ad hoc basis. Independent of the previous history of an event, it can act as a generator of other events of the same size according to a random process. We bypass the computational difficulties associated with the infinity in the occurrence rate of aftershocks as the time interval becomes shorter and shorter by the following device. In our model the probability that one event gives 'birth' to another in the time interval dt is

$$\phi(t)dt = 0 \qquad t < t_0$$

$$\phi(t)dt = (1-\kappa)\theta t_0^{\theta} t^{-(1+\theta)} dt \qquad t \geq t_0 \quad (1)$$

where t_0 can be imagined to correspond to the rupture time of an elementary earthquake; during this time the parent earthquake cannot produce other shocks. The coefficient θ specifies the 'fading memory' [Truesdell and Noll, 1965, p. 101] of the earthquake, and the coefficient κ defines the criticality of the process, which we discuss below.

Secondary shocks are assumed to occur independently of each other; these have seismic moments equal to those of all the other shocks, including the 'main' shock. In their turn, secondary shocks produce new dependent shocks according to the same law (1); the process cascades indefinitely. Since all elementary shocks are equal in this model, we do not have to apply the

Paper number 80B1069.
0148-0227/81/0808-1069$01.00

ghting factors of the lower part of Figure 1. ead we shall show in section 7 that the ndence of the rate of occurrence of fore- cks and aftershocks on magnitude difference ies as a consequence of the model we have med. Since the model is self-similar or le-independent, the size of each shock m_0 can aken to be as small as necessary if t_0 is inished correspondingly (see below). The ilting process is known in the mathematical erature as an age-dependent, continuous state, iching process [Jirina, 1958; Harris, 1963].

We have normalized the integral of the memory ction (1) over all time to be $1 - \kappa$. If $\kappa = 0$, the 'aftershocks' are said to be generated critical branching process; this means that elementary event gives birth to one endent or secondary event on the average. If >0 the process is subcritical [Harris, 1963]. virtue of the independence of all offspring number of such offspring of any event will be Poisson variable with mean $(1 - \kappa)$. The perty of a critical process which concerns us that while most Monte Carlo simulations of process may give a finite number of events, total expected number of events in such a cess is infinite. Thus the simulations of the cess are highly unstable and can lead to away cascading of seismicity. On the other d, a subcritical process always has a fir te al number of events. We call the initial ck a 'first generation' event, the events duced by this shock as second generation ats, etc. In agreement with the literature on nching processes [Harris, 1963]. We will have ourse to the index n of nth generation events. In its discrete approximation with nonzero ues of m_0 and t_0 the model can also be arded as a special case of the self-exciting nt process proposed by Hawkes [Hawkes and nopoulos, 1973, and references therein]. The features introduced in our model are the f-similarity of the occurrence of earthquakes uation 1) and the continuous state character the process. These features, taken together h that of the criticality of the branching cess, will enable us to explain in a sistent manner both the magnitude-size and e distributions of earthquakes from a set of ple assumptions. The importance of criti- lity was brought to our attention by Vere- es' [1976] earthquake branching model, which he considered as an immediate forerunner of model. The new ingredients introduced in our del are the time dependence of the rate of currence of aftershocks, and the additive aracter of the seismic moment of a series of ll events that overlap in time. Vere-Jones attributed the additive property to the frac re lengths of the individual shocks; in his del, time was not considered as a dimension of earthquake process.

4. Synthetic Seismograms

The model lends itself to Monte Carlo ulations by virtue of the digitization of the ocess through the use of the finite lower bound lues of m_0 and t_0. To facilitate the dis sion, we identify $\log_{10} m_0$ with the threshold gnitude of homogeneity of an earthquake cata- log. We take the characteristic time t_0 to be proportional to $m_0^{1/2}$ in consideration of a suggested relationship between magnitudes and earthquake rupture times [Kagan and Knopoff, 1978, Figure 3]. For example, if we set $\log_{10} m_0 = 5$ for an elementary shock and $t_0 = 1.0$ s, our simulated result can be compared with the NOAA catalog [Kagan and Knopoff, 1980b]; on the other hand, if we set $\log_{10} m_0 = 1$, and $t_0 = 0.01$ s, we match the results to the USGS catalog [Kagan and Knopoff, 1978].

Examples of such simulations are shown in the upper parts of Figures 3a and 3b for the cases $\theta = 0.5$ and 0.8, respectively. We indicate below that these values of θ are appropriate for earthquake sequences occurring at shallow and intermediate depths respectively.

The calculation is carried out as follows: we calculate the number of first generation offspring by Monte Carlo methods, which is a Poisson variable whose mean is equal to 1.0 ($\kappa = 0$); if this number is nonzero, we proceed in the same manner to calculate the number of offspring of first generation offspring, i.e., in the second generation, and so on until the whole tree of event interrelations is produced [Harris, 1963]. The time intervals between any 'parent' event and its aftershock are then simulated using (1). Finally, the resulting event sequence is sorted in time. Each subevent contributes a step function of moment m_0 to the source-time functions such as those shown in Figures 3a and 3b; these two functions are similar in appearance, since they have been produced by the same random number sequence.

The graphs of cumulative seismic moment clearly show patterns of clustering of different orders [cf. Mandelbrot, 1977, p. 100]. The source-time function appears to consist of several steps, each of which starts with a sharp onset and usually becomes more gradual after some time. This mode of behavior is to be expected in our model because the cumulative number of events in a critical branching process should increase as n^2 at the beginning of the sequence [Harris, 1963]. The time scale indicated in Figures 3a and 3b is arbitrary, so that the source-time function in the upper part of the plot can be regarded as a sequence of events occurring over several decades, over several minutes, or over several hours, as in the figure.

The synthesized source-time functions are not directly observable quantities. To compare these results with real seismograms, we must convolve the time derivative of these functions with the Green's function of ground displacement corresponding to an elementary dislocation. The resulting process is no longer self-similar because of the introduction of two characteristic times: the first is connected with the travel times of body waves and instrumental response, while the second is associated with the dispersion of surface waves and scattering processes that are manifested in the coda.

We have convolved our complex source histories with a selected theoretical seismogram; for this purpose we have used the time scale for the source function appropriate to the NOAA catalog, i.e., $\log_{10} m_0 = 5$, $t_0 = 1$ s. The theoretical seismograms for an elemental step-function, displayed in the middle picture of Figures 3a and 3b, were calculated by a program from Liao et al. [1978]. The epicentral distance in both cases is close to 7000 km; the focal depths are 0 and 140 km, respectively; the component displayed is SH. The cross section is a continental structure for the shallow source and more-or-less typical oceanic structure for the source at intermediate depth. The first case (Figure 3a) corresponds to a strike slip dislocation on a vertical fault plane; the second case is that for dip slip motion, also on a vertical fault plane. The seismograms are the result of passing the ground motion through a filter equivalent to a standard 15-15 World-Wide Standard Seismograph Network (WWSSN) seismograph. The convolution in our case is computationally simple because the kernel is convolved with a comb of delta functions.

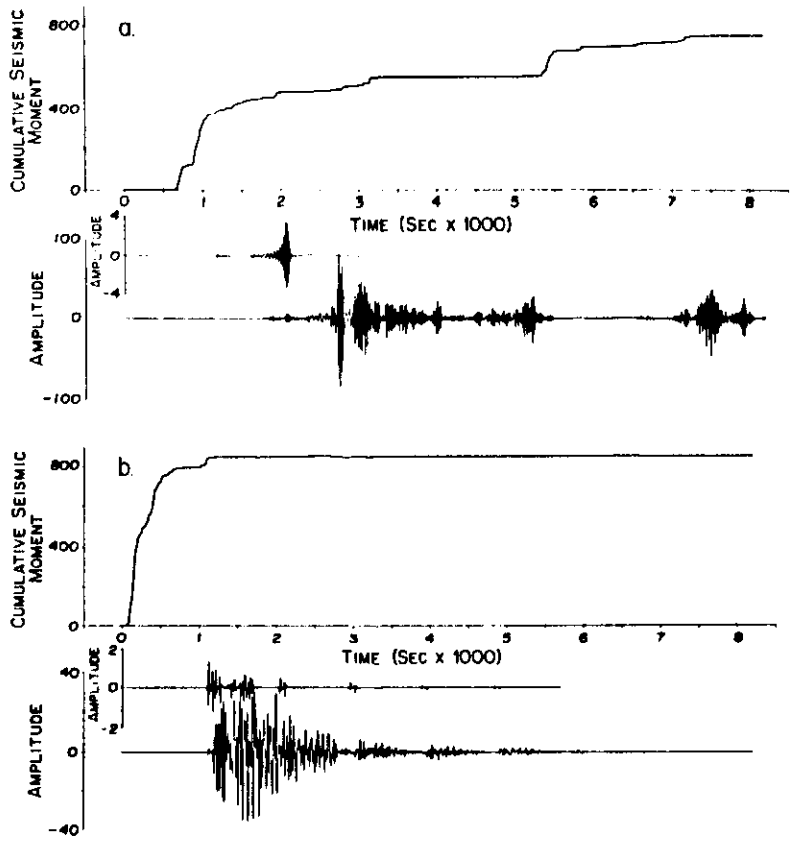

Fig. 3. Simulated source-time functions and seismograms for shallow (a) and intermediate (b) earthquake sources. The upper trace in each plot is a synthetic source-time function. The middle plot is a theoretical seismogram described in the text, and the lower trace is a convolution of the derivative of source-time function with the theoretical seismogram.

The traces in the lower parts of Figures 3a and 3b are the results of the above computation and show the complex form not atypical of recordings of strong earthquakes and differ only in one major regard. We have not introduced codas; scattering by random inhomogeneities is not taken into account in the theoretical seismograms.

In principle, these seismograms, or others generated by similar methods, could be tried out on a practitioner of the compilation of earthquake catalogs from long-period teleseismic recordings to see which discrete events, plus

associated magnitudes, will be identified. This is a formidable task and will not be undertaken at this time.

5. Simulation of Synthetic Catalogs of Earthquakes

We bypass the problem of convolution by constructing a simplified version of the seismogram for the specific purposes of this study, which are catalog simulation and analysis. For the purposes of event identification a simple envelope drawn around the highly oscillatory kernel seismogram probably suffices. Here much of the problem of identification lies in the effective description of coda waves, since the persistent coda of strong earthquakes may mask the largest amplitude arrivals due to later, smaller earthquakes. Evernden [1976] has suggested an exponential form for this envelope. If we take this point of view, then we model a complex source as yielding a seismogram that is a superposition of exponentials of different initial heights and different occurrence times; the use of the exponential envelope function greatly reduces computation cost of simulations. The envelope function is the same as an equivalent source-time function, which is a convolution of the stepwise source-time function considered above with a decaying exponential. By using the equivalent source-time function we ignore the effects of change in the length of the coda with epicentral distance.

An example of an equivalent source-time function constructed as a sum of exponentials is shown in Figure 4, where the shallow source-time function of Figure 3a is convolved with an exponential decay function with a time constant $\beta = 400$ s; this value of β corresponds roughly to that suggested for the envelope of the coda of distant shallow earthquakes [Evernden, 1976]. We can match the duration magnitude curve for individual earthquakes in the USGS catalog [Lee et al., 1972] in the magnitude range $0 < M_L < 1$ by using an exponential function with decay time β near 3.0 s. In the frequency and distance range represented by the USGS network in California we are evidently using a part of the seismograms other than the surface wave coda to generate a kernel seismogram, and consequently, a smaller value of β is called for. The values of the ratio β/t_o for the two cases are roughly the same. As we will see below, the dimensionless quantity β/t_o defines the values of the parameters used in the statistical analysis of earthquake catalogs. The fact that this ratio is approximately the same for both catalogs is consistent with the similarity of the values of the parameters that describe the aftershock sequences [Kagan and Knopoff, 1980b]. The similarity of the values of the parameters found in the statistical analysis of these earthquake catalogs seems to imply that the properties of these seismographic networks and the properties of the scattering of seismic waves in worldwide versus local seismic wave propagation are scaled in such a way as to ensure the similarity of β/t_o.

We define individual earthquakes from the equivalent source-time function by the following formal rule. We introduce a cutoff threshold,

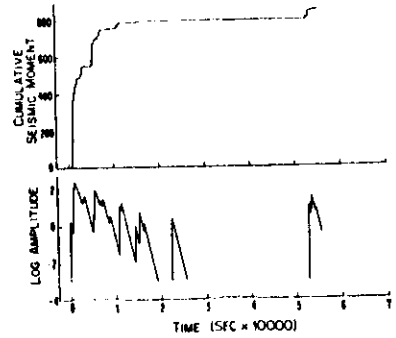

Fig. 4. Amplitude envelope in the case $\beta = \infty$ (equivalent to the simulated cumulative moment-time function) and $\beta = 400$ s. The lower amplitude scale is adjusted so that $\log_{10} m_o = 0$. The horizontal line corresponds to the amplitude cut-off level.

which is the horizontal line in Figure 4; for computational purposes we have taken this threshold M_t to be close to $\log_{10} m_o - 0.5$. Each time the trace reaches this threshold, an earthquake is presumed either to have started or stopped and thus defines the duration of an earthquake. The number of elementary events in this time interval is taken to be proportional to the seismic moment M_o of the earthquake.

We define a quantity M_β that is the logarithm of the peak of the source-time moment function convolved with decaying exponential for each burst (Figure 4). This quantity, which we call the β magnitude of an earthquake, evidently depends strongly on the value of β: if β were infinite, as in the upper curve of Figure 4, M_β will be equal to the logarithm of the total seismic moment of a simulated earthquake sequence. We have introduced this quantity by obvious analogy with conventional methods of measuring magnitudes. Our measure does not take instrumental response into account and hence is not directly comparable with conventional magnitudes. Nevertheless, the prospect of using this measure of the size of an earthquake is too tempting to bypass; below we shall show some similarities between β magnitudes and conventional magnitudes. In this paper, most of our examples are for the case $\beta = 400$ s.

The replacement of the theoretical seismogram by the exponential envelope function has certain drawbacks. At instrumental periods less than the interval between a pair of subevents the waves in the coda add incoherently, and the sum will be proportional to the square root of the number of the subevents; hence our equivalent source-time function will no longer have a simple additive property. The impact of our failure to take this effect into account on the statistics of synthetic earthquakes is twofold: First, the incoherent addition of codas will tend to reduce the overall decay time of a burst of events; if

the decay rate for the equivalent source-time function is shorter than the one we have used, some small earthquakes formerly reported as a part of a larger multiple shock event, will be reported as independent events; this increases the b value. Second, the moment-duration relation will be skewed to shorter durations for a given moment; while the duration may be changed, the β magnitude, however, will not be much affected, since the maximum of an equivalent source-time function most probably corresponds to the densest concentration of events in a cluster: the addition of these codas is more likely to be coherent because of the short time interval between these events.

The critical branching process described by (1) with $\kappa = 0$ cannot be used for numerical simulations because of the instability of this case. For some simulations of the critical process, very large numbers of events are produced; because dependent shocks are distributed in time according to the power law of (1), these events are usually concentrated in a short time interval and correspond to the occurrence of an unacceptably strong earthquake. To avoid problems connected with instabilities, stabilization was introduced into the simulation by the use of a slightly subcritical process (section 3) with $\kappa = 0.01$. To make up for the deficiency due to normalization, we introduced into our simulation a number of independent occurring elementary events which can be interpreted, for example, as representing aftershocks of earthquakes occurring before the start of the catalog. The use of a subcritical instead of a critical process also means, in effect, that a bend in the log moment-frequency curve will have been introduced at the large moment end of the curve. The bend can be parameterized by the introduction of a maximum magnitude into the magnitude-frequency relation [Knopoff and Kagan, 1977]. In our case, the subcritical branching process yields a β-magnitude-frequency distribution function that is almost linear for small magnitudes and has an increasing slope with increasing magnitude [Vere-Jones, 1976] instead of an abrupt truncation at the value of the maximum magnitude.

In the simulations we used 300 independent shocks to 'restart' the sequence due to the termination by the subcritical nature of the process; the total number of elementary events generated was usually slightly less than 100,000. The length of the simulated catalog was $10^{10} t_o$. We have only used events with magnitudes greater than $M_{co} = \log_{10} m_o + 0.5$; this effectively removes 'quantization noise' arising from our use of elementary shocks of finite size. The parameters we have used to describe the occurrence of earthquakes [Kagan and Knopoff, 1980b] are largely insensitive to variations of either M_{co} or κ, which, in the latter case, is equivalent to maximum magnitude, as noted.

An example of a simulated catalog is shown in Figure 5a; for comparison, Figure 5b shows a portion of the USGS catalog for 1976. Both catalogs appear to be similar, although USGS has seemingly more events which do not belong to an easily identifiable cluster of earthquakes. We may suppose that these shocks are connected statistically with earthquakes that occurred before the start of the section of the catalog that is displayed. In the simulated catalogs, as indicated above, these 'orphan' shocks were modeled as independent initial events. In the mathematical literature these events are called 'immigrants' [Harris, 1963].

We consider the following example to illustrate the effect of changing some of the parameters in the simulation. We generate a catalog to try to simulate the NOAA catalog by using an elementary unit of smaller size. We take $t_o' = 0.1$ s, $m_o' = 10^{-2} m_o$ and keep $\beta = 400$ s and $M_t' = 4.5$, which are defined effectively by the transmission properties of the earth and the seismographic response. To match the new catalog with our first simulation, we would have to use $\kappa = 10^{-4}$ and 3000 shocks for the purpose of restarting. The value of M_{co} could be set to $M_t' + 0.5$ or even lower because with such a small value of m_o' we need not be concerned with quantization effects; the length of the catalog is $10^{11} t_o'$ in this case. The total number of events generated would be nearly 10^7.

6. First-Order Analysis of Synthetic Catalogs

To analyze the synthetic catalogs, as with real catalogs, we first draw the β-magnitude-frequency distribution, which is the first-order moment of the process. The β-magnitude-frequency plots for several values of β are shown in Figure 6, where we have plotted $M_\beta + \log_{10} N$ as the ordinate to display more clearly small difference of the b values from unity, if there are any [Kagan and Knopoff, 1980b, Figure 2]; in this plot a horizontal line corresponds to the value $b = 1$. For $\beta = 400$ s we get b close to 0.5, which is a value close to that for the distribution of seismic moments or energies in real catalogs.

The result $b = 0.5$ for β/t large is not unexpected for these synthetic sequences, since if, for example, β is close to infinity our 'earthquake' would include almost all of the events in a critical branching process. The dis-

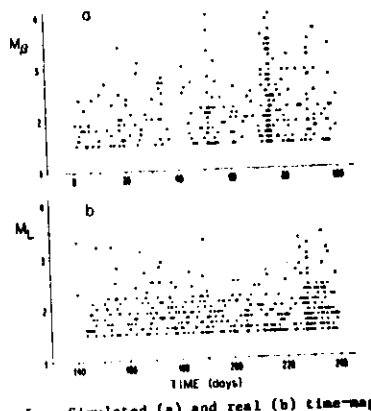

Fig. 5. Simulated (a) and real (b) time-magnitude plots of catalogs.

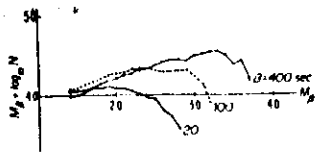

). Cumulative β-magnitude-frequency relafor synthetic catalogs produced using ent values of the time constant β.

on density of the total number N_t of ary events is proportional to $N_t^{-3/2}$ ones, 1976; Harris, 1963, Chap. I.13]; in el $\log_{10} N_t$ is a seismic moment up to a icative constant. As $\beta \to \infty$ the seisent and magnitude are equivalent. The ive distribution of magnitudes plotted hmically thus has the constant slope). In our synthetic catalogs we can e this result by considering the limiting $t_0 \to \infty$ such that $T/\beta \gg 1$, where T is gth of the catalog; in this limit, $b \to 0.5$. e use a smaller value of β/t_0, then only ll part of the branching process occurs threshold during the later parts of the ntially decaying tails; the branching s in the tail can be considered to be tical, and the corresponding b values would se [Vere-Jones, 1976]. For example, if s, then b is close to 1.0 (Figure 6). he association of this value with a similar e for surface wave magnitudes it is ng to suppose that our β magnitudes for s correspond to surface wave magnitudes. rrespondence may not be unreasonable, since y decaying exponential functions supply nt numbers of short-term aftershocks of earthquakes; the individual shocks are not fiable as discrete events under the ry circumstances of teleseismic observation range where 20 s seismic waves dominate ectrum of the signal received. Hence the f appearance of small shocks in a catalog = 400 s is likely to be less than for a g with β = 20 s, with consequent decrease b value in the former case.

The b values for synthetic catalogs with θ = 0.5 and those with θ = 0.8 and 0.9 (Table 1) are almost the same as for those for real catalogs of shallow and deep earthquakes, respectively [Kagan and Knopoff, 1980b]; the b values for deep shocks are the slightly smaller of the two. If we associate a higher β value with deep shocks, we see that a larger fraction of a deep earthquake sequence occurs in the same time interval in comparison with shallow earthquake sequences (compare Figures 3a and 3b). Thus the same reasoning that yields the dependence of b on β applies in this case as well: the value of b for deep shocks should be closer to 0.5 for our simulated catalogs.

Because of the use of an equivalent source-time function that focuses on the coda as the feature that distinguishes one earthquake from another we have effectively removed any possibility of discussing ordinary magnitudes which are strongly dependent on instrumental responses at periods much shorter than β = 400 s. If we wish to describe ordinary seismic magnitudes, we have to gain access to it through the coda. The dependence of the duration D of the earthquake record on the β magnitude is similar to that for shallow earthquakes [Kagan and Knopoff, 1978, Figure 3]

$$\log_{10} D = 0.5\, M_\beta + \text{const} \qquad (2)$$

if the time rate of occurrence of dependendent shocks varies as $t^{-1.5}$, which is appropriate for shallow shocks. We offer the conjecture that β magnitudes are simply related to ordinary magnitudes. As θ increases to 0.8 or 0.9, the value of the exponent in (2) decreases to 0.3; thus our model predicts that deep and intermediate earthquakes should have shorter wave trains than shallow earthquakes if our conjecture is correct.

Another feature that bears on our proposal that β magnitudes and surface wave magnitudes are similar, arises from comparison of the seismic moment β magnitude curve for synthetic catalogs and the moment-magnitude curve for real catalogs (Figure 7). In the synthetic case we have used $\log_{10} n_u = 5$ or $M_{cu} = 5.5$ to correspond to our estimates for the NOAA catalog. The reference curve for the case of real catalogs is that proposed by Aki [1972]. The similarity is strong.

TABLE 1. Values of Parameters for Simulated Catalogs

	Simulation Numbers					
	1	2	3	4	4	4
	0.5	0.5	0.5	0.5	0.8	0.9
	0.622±0.067	0.634±0.057	0.683±0.075	0.642±0.065	0.589±0.089	0.602±0.091
	1.154	1.157	1.170	1.159	1.145	1.149
	22.12	30.91	18.93	23.89	12.24	11.89
	1.168	1.148	1.157	1.172	1.155	1.154
	11.19	11.22	9.77	11.67	10.79	11.02
	0.06041	0.05406	0.06990	0.03968	0.03943	0.03816
	0.03529	0.02812	0.01652	0.01845	0.00565	0.00089
	0.595	0.635	0.647	0.675	0.474	0.582
	1.096	1.150	1.192	1.168	1.109	1.172
	0.088	0.147	0.127	0.081	0.036	0.053
	0.605	0.657	0.492	0.478	0.104	0.024
κ)	2.8	2.8	2.7	3 0	3.8	4.0
	294	408	244	314	166	160
	701.0	1274.2	456.0	733.2	57.6	25.0
	3.44	4.51	2.70	3.37	0.50	0.23

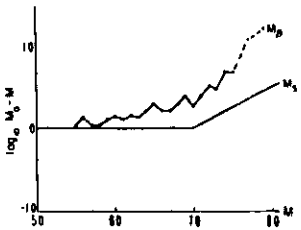

Fig. 7. Seismic moment versus magnitude relations. The bold line is $\log_{10} M_0 - M_S$ as a function of M [Aki, 1972]. The irregular curve is $\log_{10} M_0 - M_\beta$ as a function of M_β derived from catalog synthesis.

7. Earthquake Interaction Analysis

To study the second-order properties of simulated catalogs, which correspond to pairwise interaction of earthquakes, we can use the same maximum likelihood optimization procedures that were applied to real catalogs [Kagan and Knopoff, 1978, 1980b]. The values of the parameters in the optimization for the simulated catalogs are shown in Tables 1 and 2 in a form comparable to Tables 2 and 3 of Kagan and Knopoff [1980b]. For θ = 0.5, values of the parameters, and especially ν_+ are obtained that are similar to those for catalogs of shallow earthquakes. The quantities ν_+ correspond to the average number of aftershocks or foreshocks to be expected if the magnitude difference between a main shock and a dependent shock is $\Delta M \le 1.0$ [Kagan and Knopoff, 1978]. The values of α and γ in Table 1 correspond roughly to the parameters a and b in the magnitude-frequency relation; $b = 10\log_{10}\gamma$ for independent shocks, and for a Poissonian model $b_o = 10\log_{10}\gamma_o$ [for definitions of α, γ, α_o and γ_o, see Kagan and Knopoff 1978]. The parameter $M_{\beta(max)}$ in this table refers to the maximum β magnitude of all earthquakes synthesized in a given catalog, while n is the total number of the events in the catalog.

Foreshocks were not introduced explicitly in the model of (1). Nevertheless they make their appearance in the simulated catalogs (Tables 1 and 2), and they have time and β magnitude distributions similar to real foreshocks. This supports our assertion [Kagan and Knopoff, 1978] that both foreshocks and aftershocks are a manifestation of essentially the same process, namely, the stochastic interaction of earthquakes. Simply stated, if the second earthquake of a pair of interrelated shocks happens to be larger than the first, we call the first member of the pair a foreshock. From the values of ν_+ in Table 1 the number of cases for which the above possibility is encountered in simulated catalogs is in good agreement with the corresponding number for real catalogs.

Although all events were produced by the same stochastic mechanism, foreshocks and aftershocks seem to have different β magnitude distributions as reflected in the values of c_- and c_+, respectively: the number of dependent events in the β magnitude interval dM_β, is proportional to $c^{10\Delta M_\beta} dM_\beta$. The values of c_+ in real catalogs [Kagan and Knopoff, 1980b] are approximately similar to the values for synthetic catalogs, although the values of c_- in the simulated catalogs are lower than their real counterparts.

The greatest difference between the second-order properties of simulated and real catalogs relate to the values of the branching rate μ for short-time aftershocks. The values of μ in aftershock time intervals 1 and 2 are significantly higher for the simulated catalogs than the corresponding estimates for real earthquakes [for definition of time intervals see Kagan and Knopoff 1978, 1980b]. This discrepancy may be connected with the incomplete identification of weak shocks in the wake of strong main events in real earthquake catalogs. In our maximum likelihood optimizations we have excluded earthquakes which occurred a short time after the main shocks from both the real and simulated catalogs [Kagan and Knopoff, 1978, 1980b]. The residual real catalogs may still be biased due to the possible failure to take into account some weak aftershocks which occur at the shortest time intervals (1 and 2).

The partial absence of short time aftershocks in real catalogs may also explain the higher values of the likelihood function $\ell - \ell_0$ [Kagan and Knopoff, 1978] for simulated catalogs (Table 1) and the lower values of the coefficient c_- in the simulated compared to real catalogs. If so, then our earlier result that $c_- = 1/c_+$ [Kagan and Knopoff, 1978] may be coincidental. The entry 1/n in Table 1 shows the average amount of information in a catalog in units of bits per earthquake [Kagan and Knopoff, 1977]. We have noted earlier that the values of $\ell - \ell_0$ and 1/n

TABLE 2. Values of Branching Coefficient $\mu \times 10^5$ in Simulated Catalogs

	Foreshock Time Intervals								
	9	8	7	6	5	4	3	2	1
θ = 0.5	1108	111	389	209	102	130	709	869	1974
θ = 0.8	0	1595	0	0	1501	0	0	868	0
θ = 0.9	130	2043	0	0	1031	0	0	0	612
	Aftershock Time Intervals								
	1	2	3	4	5	6	7	8	9
θ = 0.5	722	682	400	212	64	158	39	48	162
θ = 0.8	184	137	70	0	0	0	41	133	0
θ = 0.9	35	23	0	0	10	0	0	21	0

Entries for θ = 0.5 are averages of μ for four simulations (see Table 1).

12

are determined mostly by the short-time interval aftershocks [Kagan and Knopoff, 1977, 1978]; this is due to our use of a maximum likelihood procedure which is influenced most by the high-density regions of the population.

The coefficients describing the time interaction between shocks ν_+ are significantly different for different values of θ and hence for different depths, a result that is similar to our observations for real catalogs [Kagan and Knopoff, 1980b]. We have already commented above that both the synthetic and real catalogs have b values that are essentially independent of depth.

The model has properties that are in excellent agreement with those of catalogs of shallow earthquakes; this agreement is all the more remarkable, since we have been able to generate almost all the known time-magnitude statistical features of shallow earthquake catalogs with only four parameters θ, $m_0^{1/2}/t_0$, θ/t and $(\log_{10} m_0 - M_t)$. Two additional parameters, κ and M_{co}, play a relatively insignificant role as determinants of the statistical properties of the result, as long as κ is small. We note that the magnitude-frequency relation is derived in our model from the inverse power law memory function of an earthquake process (1) and the assumption of the branching property of the process. Thus the two basic laws of statistical seismology, namely, Omori's law and the magnitude distribution, have been shown to be nonindependent; the second is a consequence of the first.

With regard to seismicity at greater depth, unfortunately, we have only two statistical results with which to compare: the magnitude-frequency relation and the upper bound for the rate of earthquake interaction [Kagan and Knopoff, 1980b]. It is possible, in principle, that the coincidence of predictions from the model with these two features is fortuitous.

8. Implications for the Problem of Seismic Risk

Our model suggests a simple formula in regard to earthquake risk prediction: the average predicted seismicity at a time t immediately after the end of a catalog can be estimated as

$$\lambda(t) = \text{const} \sum_i M_{oi}(t - t_i)^{-3/2} \qquad (3)$$

where M_{oi} is the seismic moment of the ith earthquake in the catalog and t_i is the time of this earthquake; the normalization coefficient is given in (1).

To calculate the seismic risk at some future time t', we must take into account not only the influence of earthquakes in the existing catalog (3) but also the contribution of shocks which would have occurred in the time interval (t'-t). The latter part can be evaluated, for example, by Monte Carlo simulations of several possible extrapolations of the process from t to t' and then by averaging these simulations. The uncertainty in the estimate of $\lambda(t')$ can be found by the same procedure.

To illustrate formula (3), suppose that there are two earthquake faults such that the only available information is one earthquake on each fault. We suppose that one of these earthquakes had a magnitude close to 8.0 ($\log_{10} M_o = 28$) and occurred about 300 years ago (10^{10} s), and in the other case we take $M = 3.0$ ($\log_{10} M_o = 22$) and assume that it occurred about 12 days ago (10^6 s); both of these faults have equal probabilities of producing a new shock 'today.' If we assume for simplicity that no new earthquakes have occurred on these faults one year from 'now,' the probabilities that each would produce a new earthquake differ drastically: that due to the second is 185 times less than that due to the first.

We consider the implications of the self-similarity of the seismic process for estimating long-term seismic risk parameters. If we calculate the recurrence time of an earthquake process having a conditional rate of occurrence varying as $t^{-(1+\theta)}$, we find that the average recurrence time is infinite for $1 \geq \theta > 0$ [Mandelbrot, 1977]. It can be argued that the power law distribution may not be valid for very long time intervals. We know that the spatial distribution of earthquakes [Kagan and Knopoff, 1980a] loses its self-similarity at distances greater than 2000 or 3000 km. At present we do not have techniques for estimating the corresponding time scale of disappearance of self-similarity, if there is any; it may even be as long as the time scale of mantle convection.

The infinite recurrence time of earthquakes means that the earthquake process is nonstationary. It is of interest to note that some other natural processes exhibit the same nonstationary behavior [Mandelbrot and Wallis, 1969].

Our model implies that almost all earthquakes are statistically and causally interdependent, a conclusion that contradicts attempts to divide the full catalog of earthquakes, either into sets of independent or main sequence events or into sets of dependent events (aftershocks and foreshocks). If this picture applies even for the strongest earthquakes, and our results in the previous sections and elsewhere seem to confirm this, then all earthquakes occur in superclusters with very long time spans which may exceed the time spans of all the earthquake catalogs we have at our disposal.

A partial but qualitative confirmation of this possibility can be found in the historical catalogs of China [Lee et al., 1976; York et al., 1976] and the Middle East [Ambraseys, 1971; Allen, 1975]; in these catalogs, periods of high seismic activity lasting several centuries are interspersed with periods of significantly lessened seismicity. If even longer fluctuations of activity also occur, we are simply unable to identify them in catalogs of only (sic) a few hundred or a few thousand years duration. These periods of seismic activity might correspond to the lifetime of an active fault; on a geological time scale, even major tectonic features have a limited lifetime, since they are replaced after long intervals by other tectonic features.

In summary, from all of these arguments we assert with high probability that the statistical moments of the seismic historical process do not at present provide us with an instrument to evaluate the seismic risk in the very distant future. In the catalogs presently available to us, seismicity may have a peak (or it can have a minimum as well) in recent centuries of seismic activity; our formulas for earthquake interaction (1) and (3) do not have a characteristic period; hence they cannot be used for long-term forecasting. But such risk predictions may not be too important, since in practice we only need estimates of seismic risk for a maximum period of, let us say, the next 50 to 100 years, and these estimates can be obtained by an extension of the methods discussed in this paper.

Acknowledgements. This research was supported by grant PFR 77-24742 of the Directorate for Applied Science and Research Applications (ASRA) of the National Science Foundation. We are grateful to F. Schwab for providing us with theoretical seismograms and useful discussion. We also extend our thanks to D. Vere-Jones for valuable discussion and comments. We are grateful to two referees for their useful remarks. Publication No. 2044, Institute of Geophysics and Planetary Physics, University of California, Los Angeles.

References

Aki, K., Scaling law of earthquake source time-function, Geophys. J. R. Astron. Soc., 31, 3-25, 1972.

Allen, C. R., Geological criteria for evaluating seismicity, Geol. Soc. Am. Bull., 86, 1041-1057, 1975.

Ambraseys, N. N., Value of historical records of earthquakes, Nature, 232, 375-379, 1971.

Evernden, J. F., Study of seismic evasion, III, Bull. Seismol. Soc. Am., 66, 549-592, 1976.

Harris, T. E., The Theory of Branching Processes, 230 pp., Springer, New York, 1963.

Hawkes, A. G., and L. Adamopoulos, Cluster models for earthquakes -- Regional comparisons, Bull. Int. Statist. Inst. 45 (3) 454-461, 1973.

Jirina, M., Stochastic branching processes with continuous state space, Czech. Math. J., 8, 292-313, 1958.

Kagan, Y., and L. Knopoff, Earthquake risk prediction as a stochastic process, Phys. Earth Planet. Inter., 14, 97-108, 1977.

Kagan, Y., and L. Knopoff, Statistical study of the occurrence of shallow earthquakes, Geophys. J. R. Astron. Soc., 55, 67-86, 1978.

Kagan, Y. Y., and L. Knopoff, Spatial distribution of earthquakes: The two-point correlation function, Geophys. J. R. Astron. Soc., 62, 303-320, 1980a.

Kagan, Y. Y., and L. Knopoff, Dependence of seismicity on depth, Bull. Seismol. Soc. Am., 70, 1811-1822, 1980b.

Knopoff, L., and Y. Kagan, Analysis of the theory of extremes as applied to earthquake problems, J. Geophys. Res., 82, 5647-5657, 1977.

Lee, W. H. K., R. E. Bennett and K. L. Meagher, A method of estimating magnitude of local earthquakes from signal duration, Geol. Surv. Open File Rep. U.S., 28 pp., 1972.

Lee, W. H. K., F. T. Wu, and C. Jacobsen, A catalog of historical earthquakes in China compiled from recent Chinese publications, Bull. Seismol. Soc. Am., 66, 2003-2016, 1976.

Liao, A. H., F. Schwab, and E. Mantovani, Computation of complete theoretical seismograms for torsional waves, Bull. Seismol. Soc. Am., 68, 317-324, 1978.

Mandelbrot, B. B., Fractals: Form, Chance and Dimension, 365 pp., W. H. Freeman, San Francisco, Calif., 1977.

Mandelbrot, B. B., and J. R. Wallis, Some long-run properties of geophysical records, Water Resour. Res., 5, 321-340, 1969.

Trifunac, M. D., and D. E. Hudson, Analysis of Pacoima Dam accelerogram, in San Fernando, California, Earthquake of February 9, 1971, vol. 3, pp. 375-391, U.S. Department of Commerce, Washington, D. C., 1973.

Truesdell, C., and W. Noll, The non-linear field theories of mechanics, Encyclopedia of Physics, vol. III/3, 602 pp., Springer, New York, 1965.

Vere-Jones, D., A branching model for crack propagation, Pure Appl. Geophys., 114, 711-725, 1976.

York, J. L., R. Cardwell, and J. Ni, Seismicity and quarternary faulting in China, Bull. Seismol. Soc. Am., 66, 1983-2001, 1976.

(Received February 27, 1980;
revised May 27, 1980;
accepted June 11, 1980.)

13

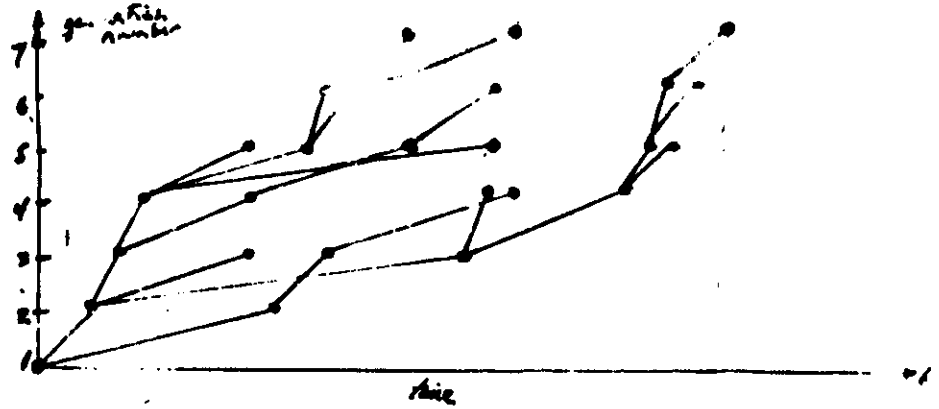

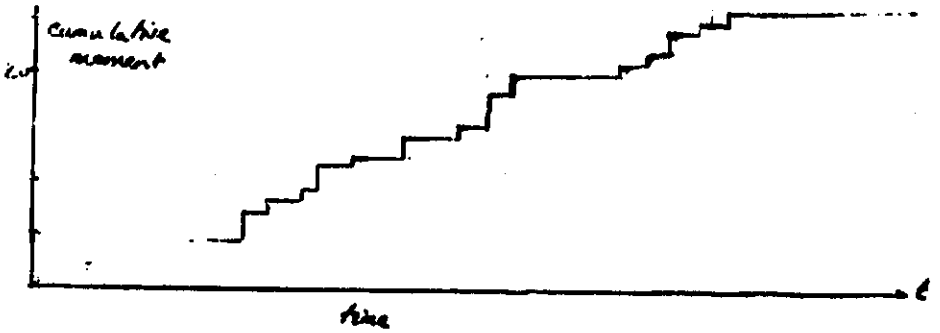

random process generates a series of impulses in which the ... dren are the same size as the parents, at the instant the ... are born.

... can take each of these impulses and convolve ... with a synthetic seismogram, as shown in the next transparency. ... produces a pretty good seismic record. What would a ... seismologist read as individual earthquakes in such a ... ord? Two events or three, or 800? We simplify ... problem by trying to simulate computationally what ... a seismograph does visually. We note that the fir... Bill ... recovered by ... envelope ... changes in ... rapidly.

Time sequence

if $n \sim \frac{1}{t^{1+\theta}}$, $n \sim \int_0^\infty \frac{dt}{t^{1+\theta}} \to \infty$

so Let Prob eg. in $dt = 0 \quad t < t_0$

Critical Branching Process $= \frac{k}{t^{1+\theta}} \quad t > t_0$, $\theta > 0$

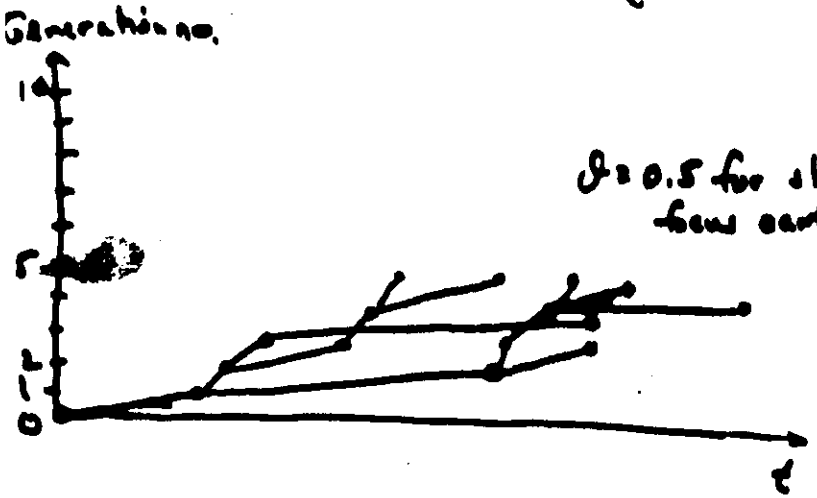

$\theta = 0.5$ for shallow focus earthquakes

Normalization k so that one event has unit prob. of generating one offspring in finite time.

1. Critical Branching Process

Ref.
Kegan & Knopoff.
J.G.R. 86 (4401) 2002.

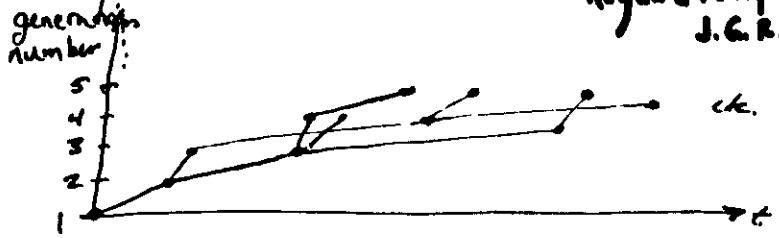

Prob that one event gives "birth" to another event in time interval dt is

$$\phi(t)dt = 0 \quad \text{for } t < t_0$$

$$= (1-K)\mu_0^{\alpha} \frac{dt}{t^{1+\alpha}} \quad \text{for } t > t_0$$

All elementary shocks assumed equal

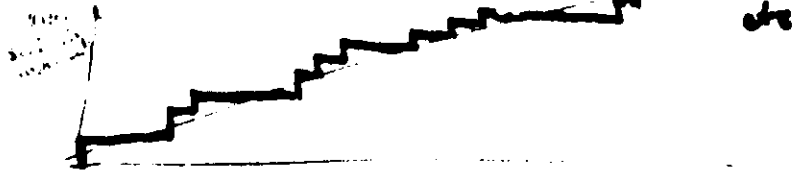

If $K = 0$ then each event gives rise to one offspring (initial mean) on the average in infinite time

for $0 < K < 1$ the process is subcritical.

for critical process mean time interval between shocks may be ∞.

For subcritical process, finite no. of shocks.

* Self-similarity Assumed

If $\beta \sim 0.5$ (shallow eqs)
~ 0.8 (deformed eqs.)

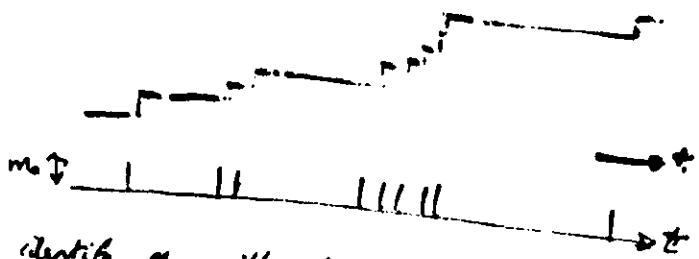

identify m_0 with threshold ~~magnitude~~ moment of detectability of network (i.e. threshold of homogeneity).

If $m_0 \sim 10^5$, $t_0 = 1$ sec (Nobbs catalog)

$m_0 \sim 10^1$, $t_0 \sim 10^{-2}$ sec (USGS central California)

Now convolve (I) with transfer function for elastic medium (Synthetic Seismogram)

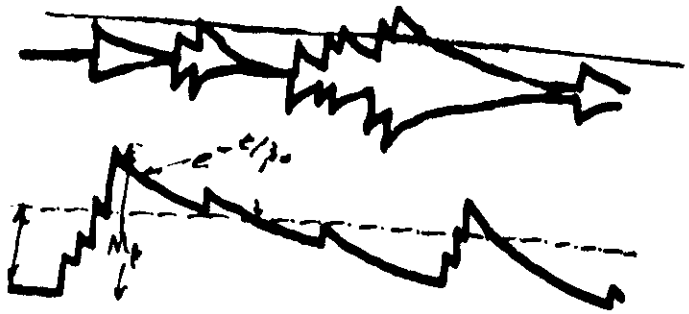

For USGS catalog, we use

$\beta_0 \sim 400$ sec (Δ ≈ 7 miles)

$M_p = 10^{4}$ WWSSN 15-sec LP seismograph

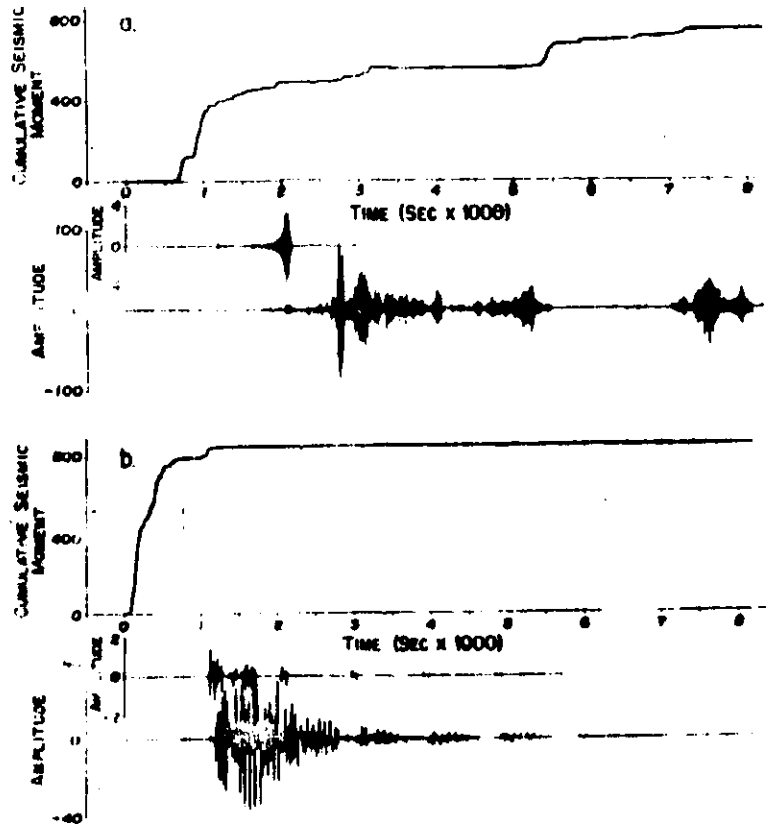

Fig. Simulated source-time functions and seismograms for shallow (a) and intermediat (b) earthquake sources. The upper trace in each plot is a synthetic source-t.. e functions. The middle plot is a theoretical seismogram described in the text, and the lower trace is a convoluti-- of the derivative of source-time function with the theoretical seismogram.

3 (1) dimensionless parameters

θ (in process of fixing)

$\bar{M}/M_0$

$t_0 \beta$

K (omori factor)

M_0 = unit moment of each event

$\bar{M}$ = threshold of detectability

t_0 = "dead time" in branching process

β^{-1} = instrumental time constant

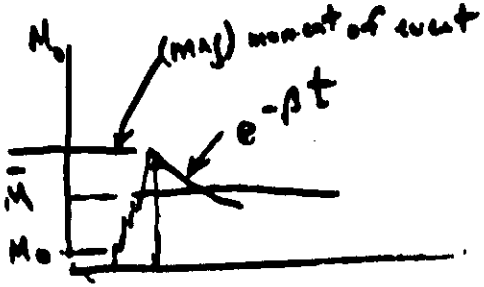

This model generates:

1. log frequency vs log moment (magnitude) relation
2. Omori law of aftershocks $N(\Delta N \text{ cond}) \sim \frac{1}{t}$
3. Magnitude - coda relation
4. Foreshocks: $1/t$

$\lambda M/$

rotation on a sphere
(3 rotations)
(Hamilton)

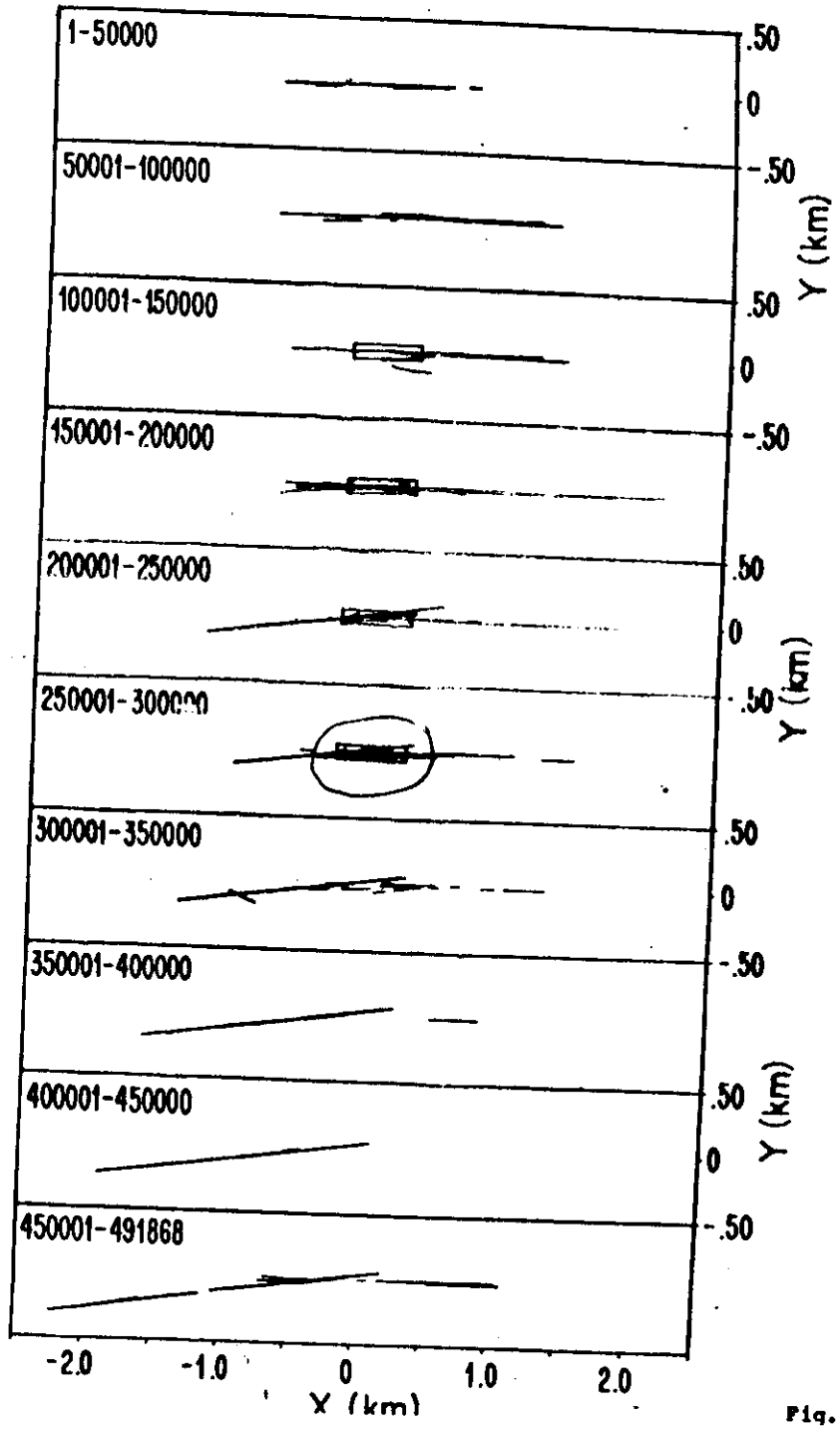

Fig. 7a

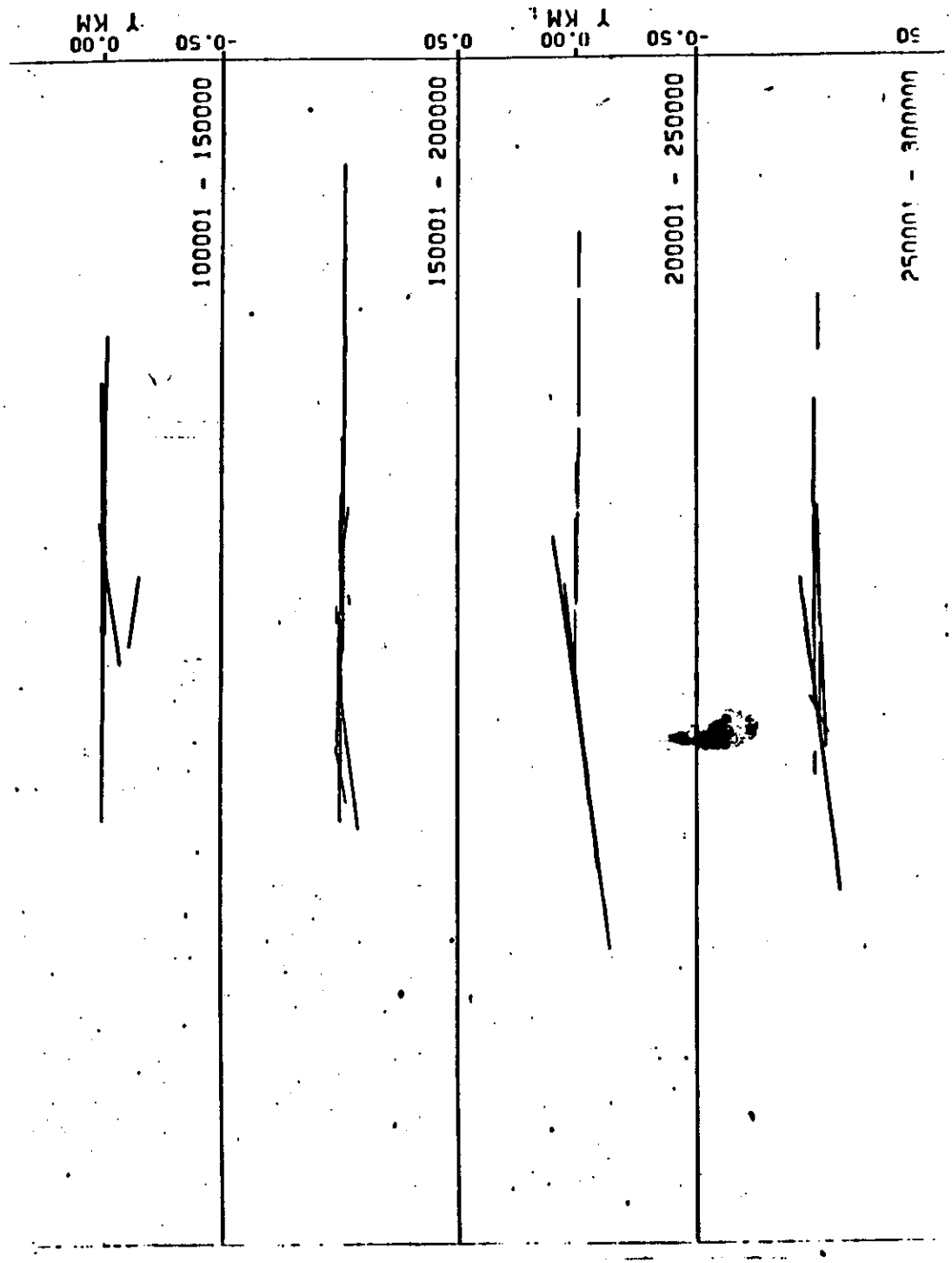
100001 - 150000
150001 - 200000
200001 - 250000
0.50
0.00
-0.50
Y KM

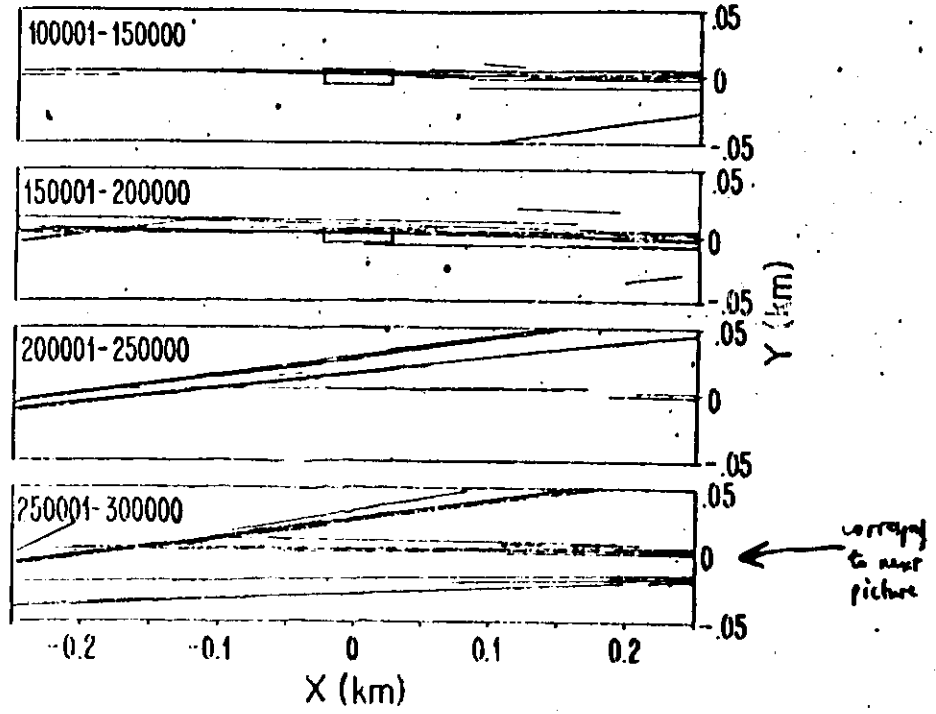
100001-150000
150001-200000
200001-250000
250001-300000
.05
0
-.05
Y (km)
-0.2
-0.1
0
0.1
0.2
X (km)
corresponds to next picture

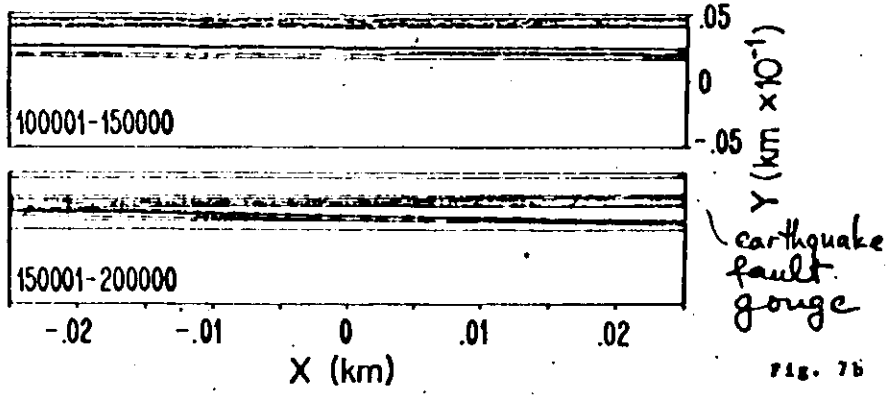
100001-150000
150001-200000
.05
0
-.05
Y (km x10⁻¹)
-.02
-.01
0
.01
.02
X (km)
earthquake fault gouge

Fig. 7b

The problem is to identify foreshocks.

Prob. that one earthquake occur after another has occurred at τ_{ab} is

$$\psi_\tau \sim \left(\frac{t_M}{\tau_{ab}}\right)^{\frac{1}{2}} \left(\frac{M}{M_a}\right)^{\mu_B}$$

M moment of eq.

t_M : scale time for eq with moment M

for cont. Calif. $t_M = 8.5 \times 10^{-3}$ days

for $M = 10^{28.4}$ ($m_b \cong 4.4$)

$t_M \propto M^{1/3}$

μ_B ave. over $M = 10^{18.6}$ ($m_b = 1.5$)

Dist. prob

$$\psi_x \sim \frac{1}{\sqrt{2\pi}\,\sigma} e^{-\left(\frac{x-x_i}{\sqrt{2}\,\sigma}\right)^2}$$

($\sigma \cong 0.5$ km for $M = 10^{24.4}$)

$$\psi \sim \psi_x \psi_t$$

We map San Andreas fault eqs. onto a line surface by

1974–77,

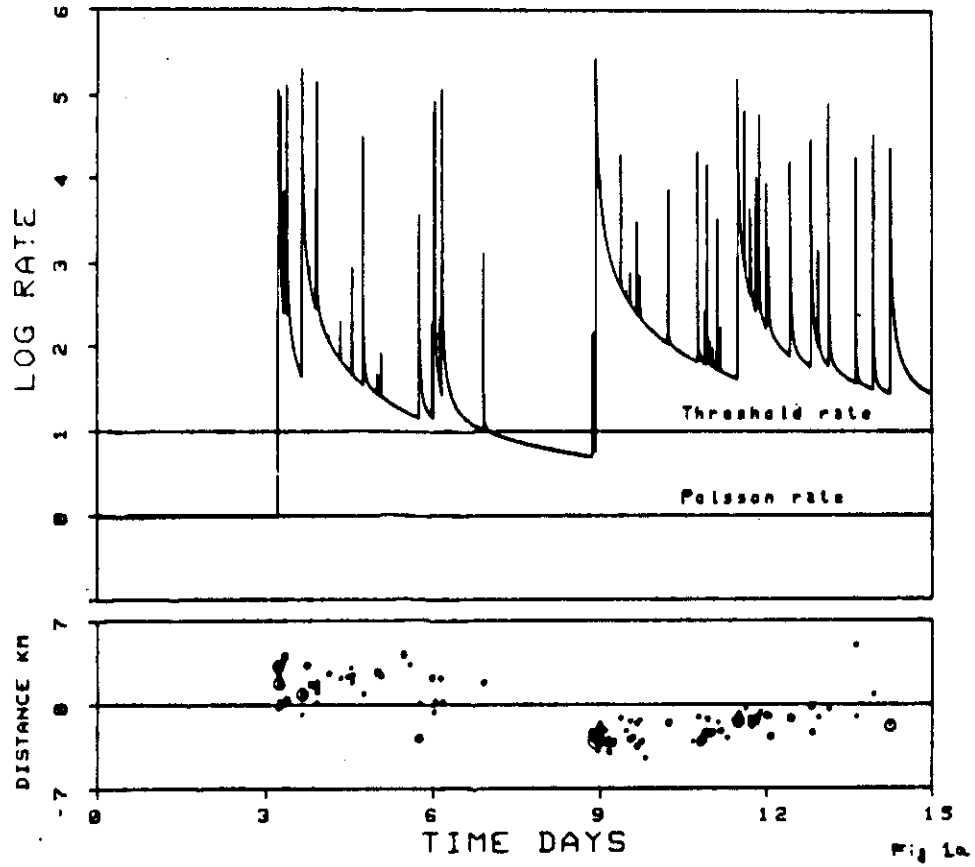

Fig 1a

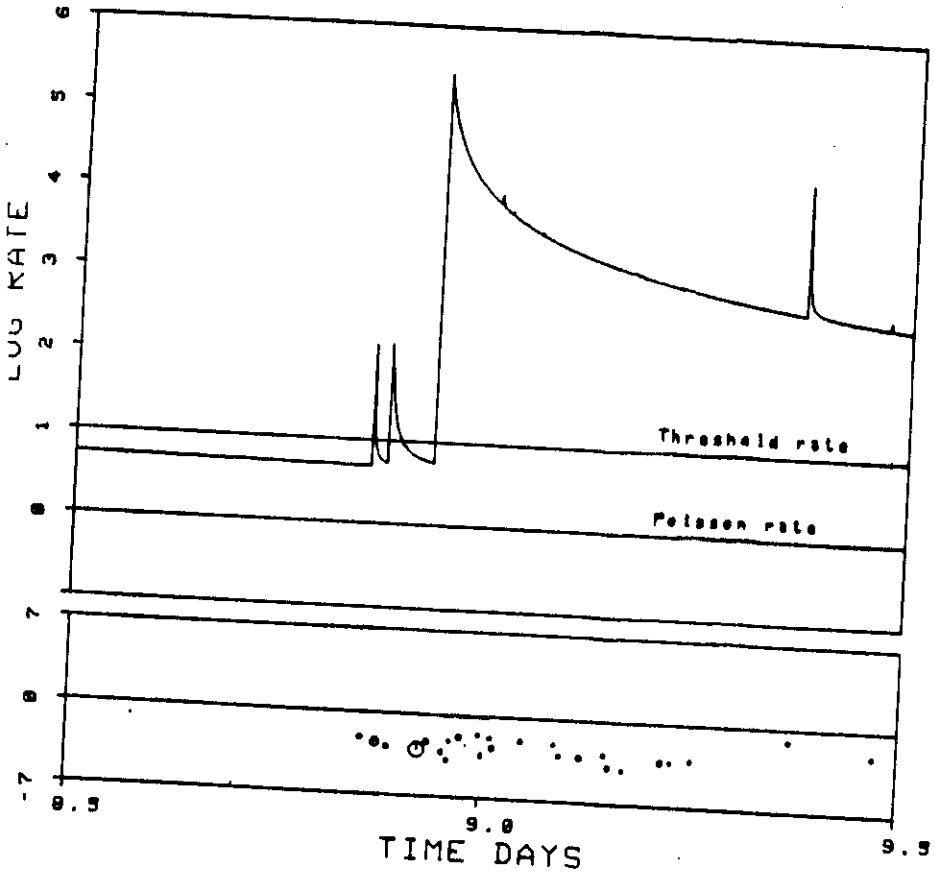
LOG RATE
Threshold rate
Poisson rate
TIME DAYS

Fig. 16

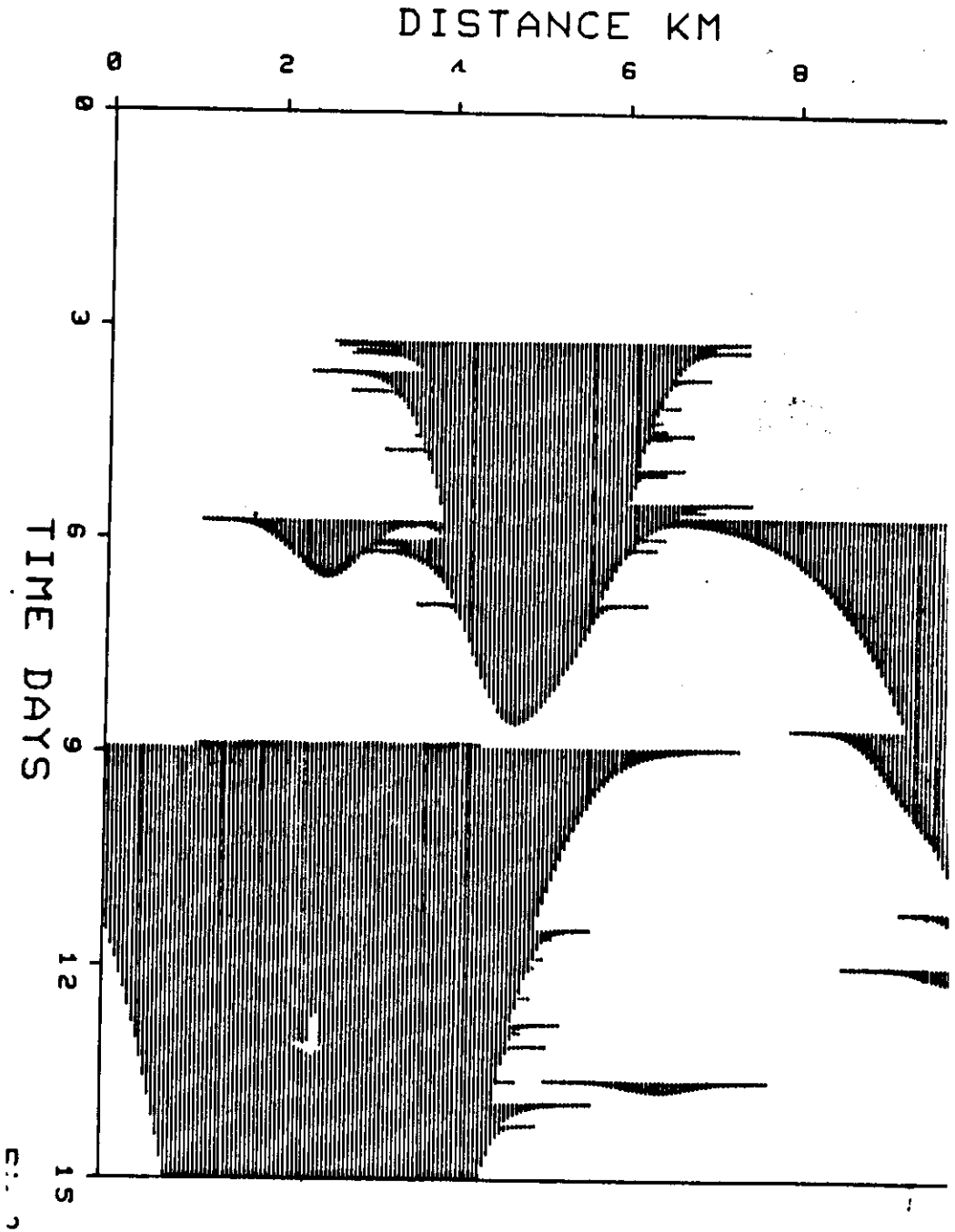
DISTANCE KM
TIME DAYS

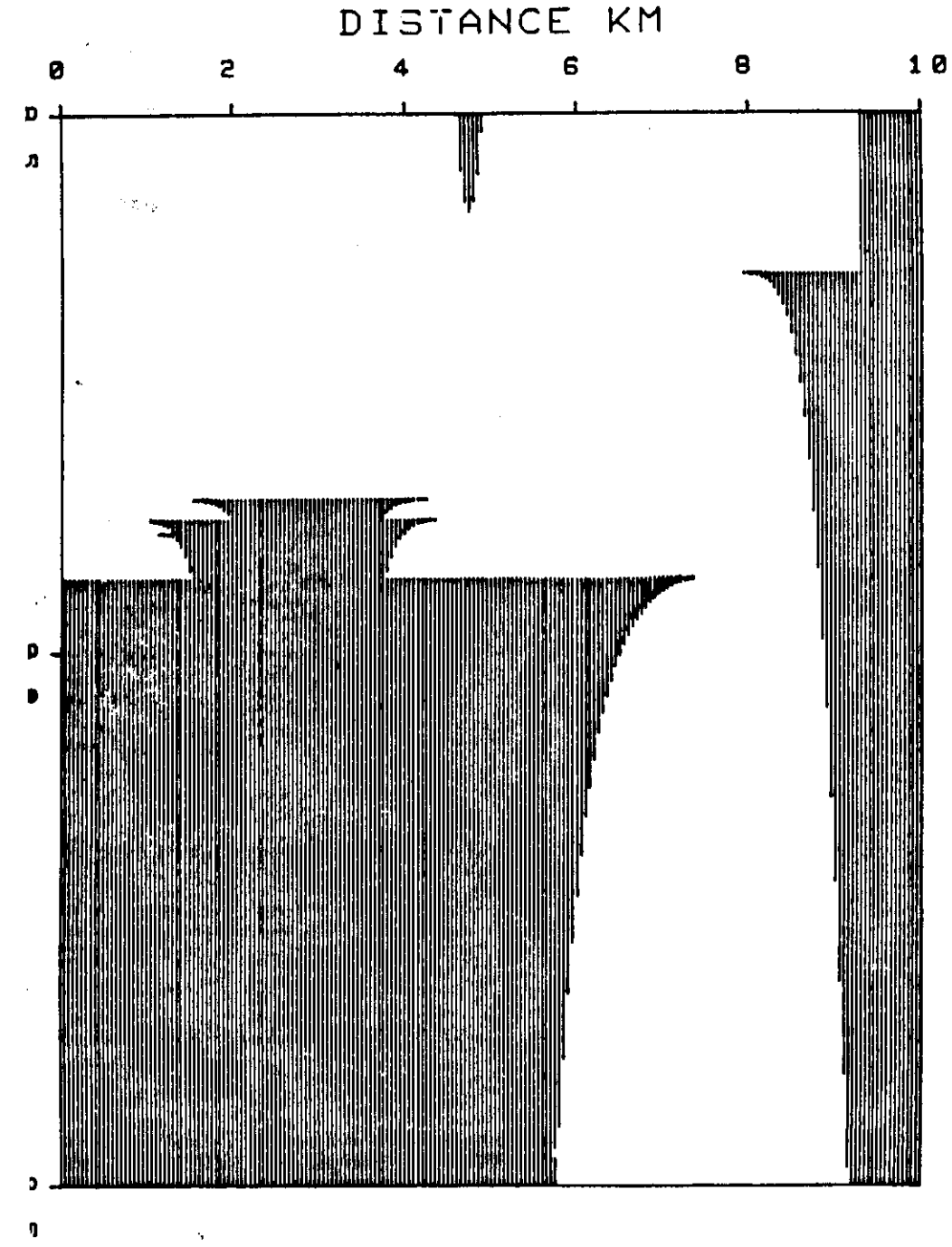

for threshold rate, $10^{-3} = R$

size = 1.5×10^{-4} of total area

40% of 58 mainshocks with $M_L \geq 3.5$

24% of 21 " " " " 4.0

occur in the swarms

for R rate of smaller earthquakes $\sim Y_3$

alarm placed for time $\frac{0.0154 \cdot 10^{\frac{2}{3} M_L}}{(R)^{\frac{1}{3}}}$ for F = 0

Next strong earthquake prob.

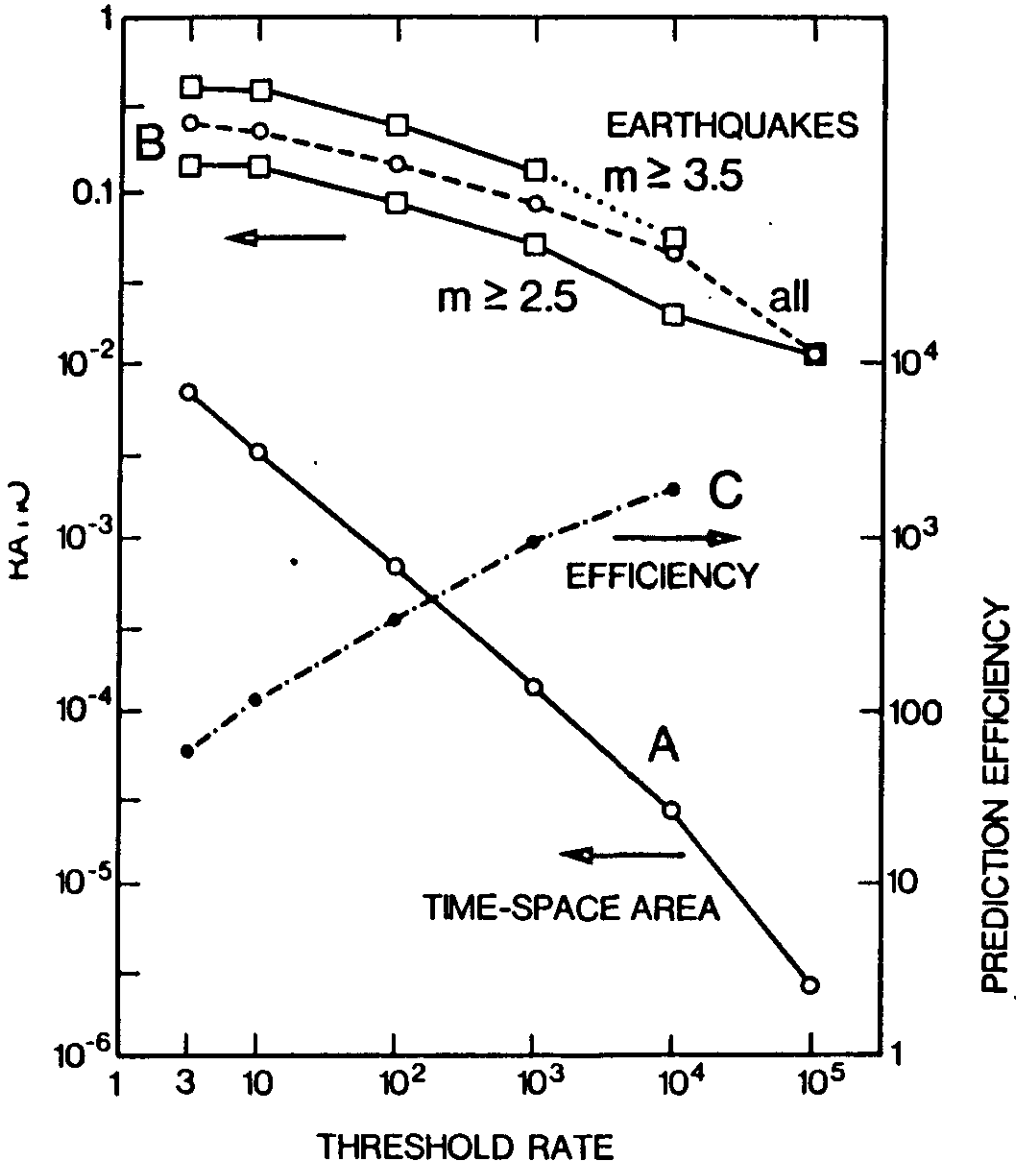

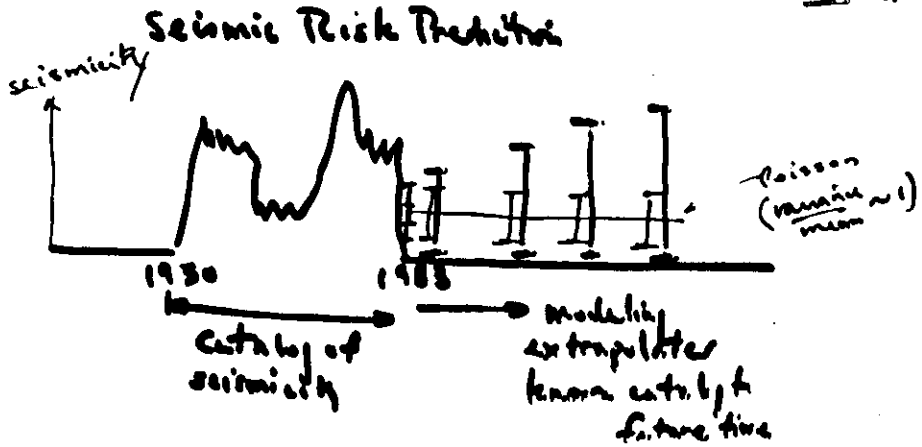

(if seismicity interactive (non-independent), then mean predictions are about the same as for Poisson model, but variances greater. In many of our models (because big gaps) variances may be more than two times as large.)

Stochastic

2-D Anharmonic Trans

Dynamical system

Quasistatic

chemical kinetics

fluids

4 d.o.f. $\frac{dG_1}{dG_2}$ k, dt, du

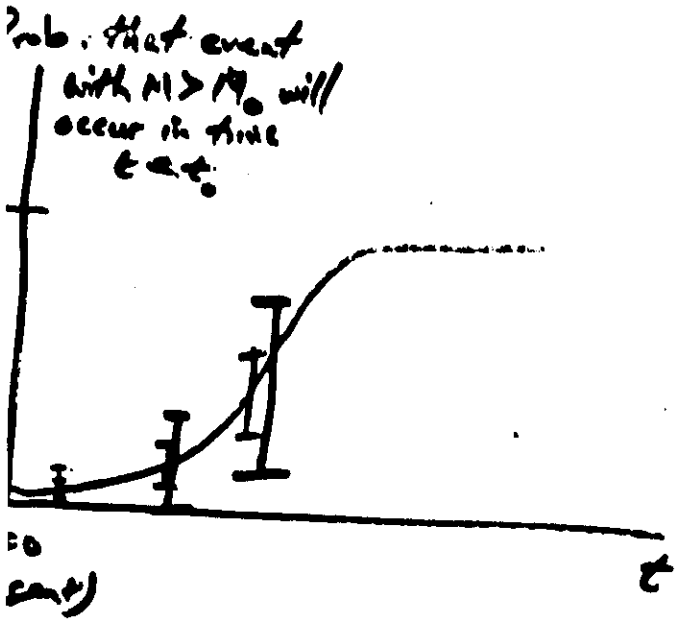

I Poisson

I $\forall t$

The Triangle Billiard

$r = \frac{1}{\pi} \tan^{-1} \sqrt{\frac{m_1}{m_2}}$

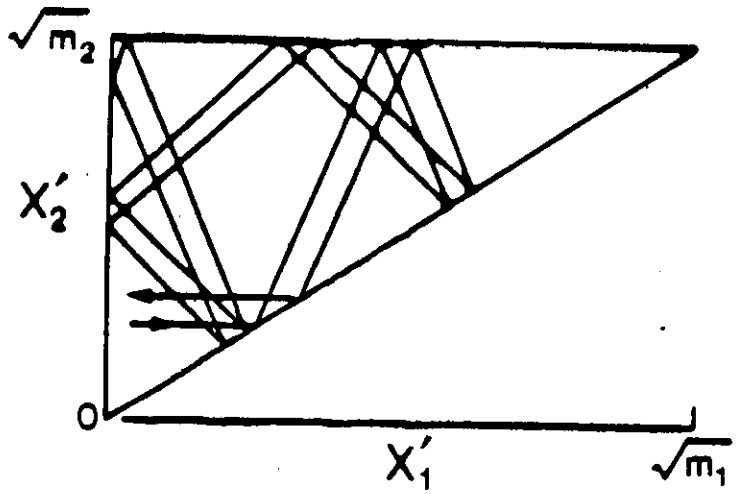

Fig. 1

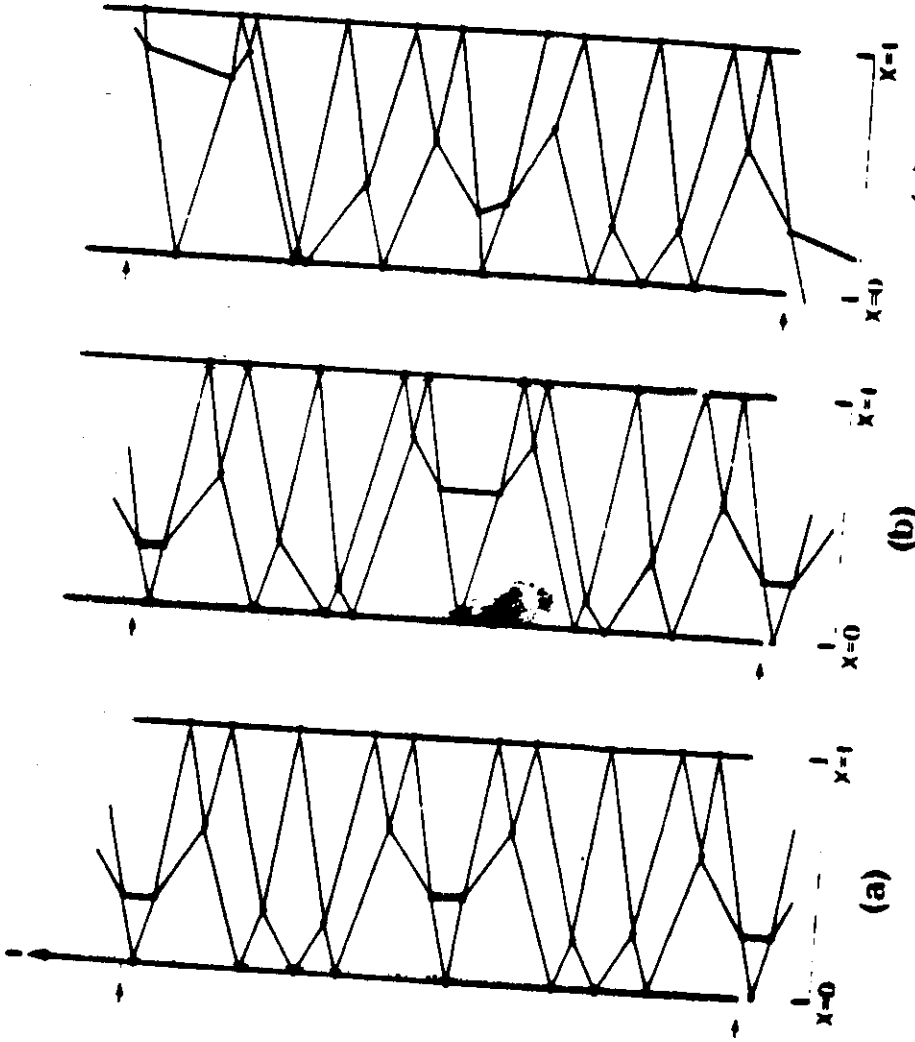

Fig. 2

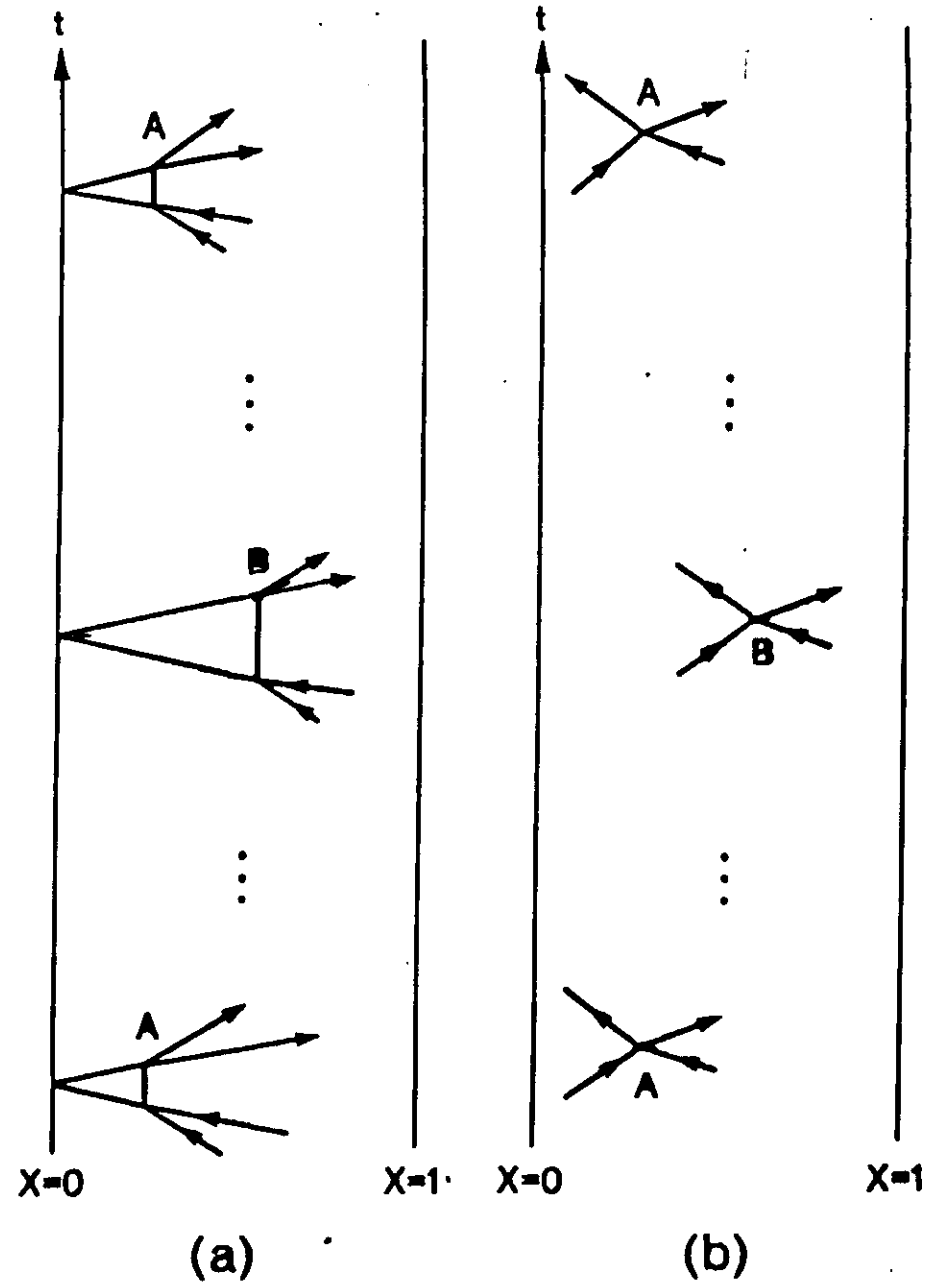

Fig. 3

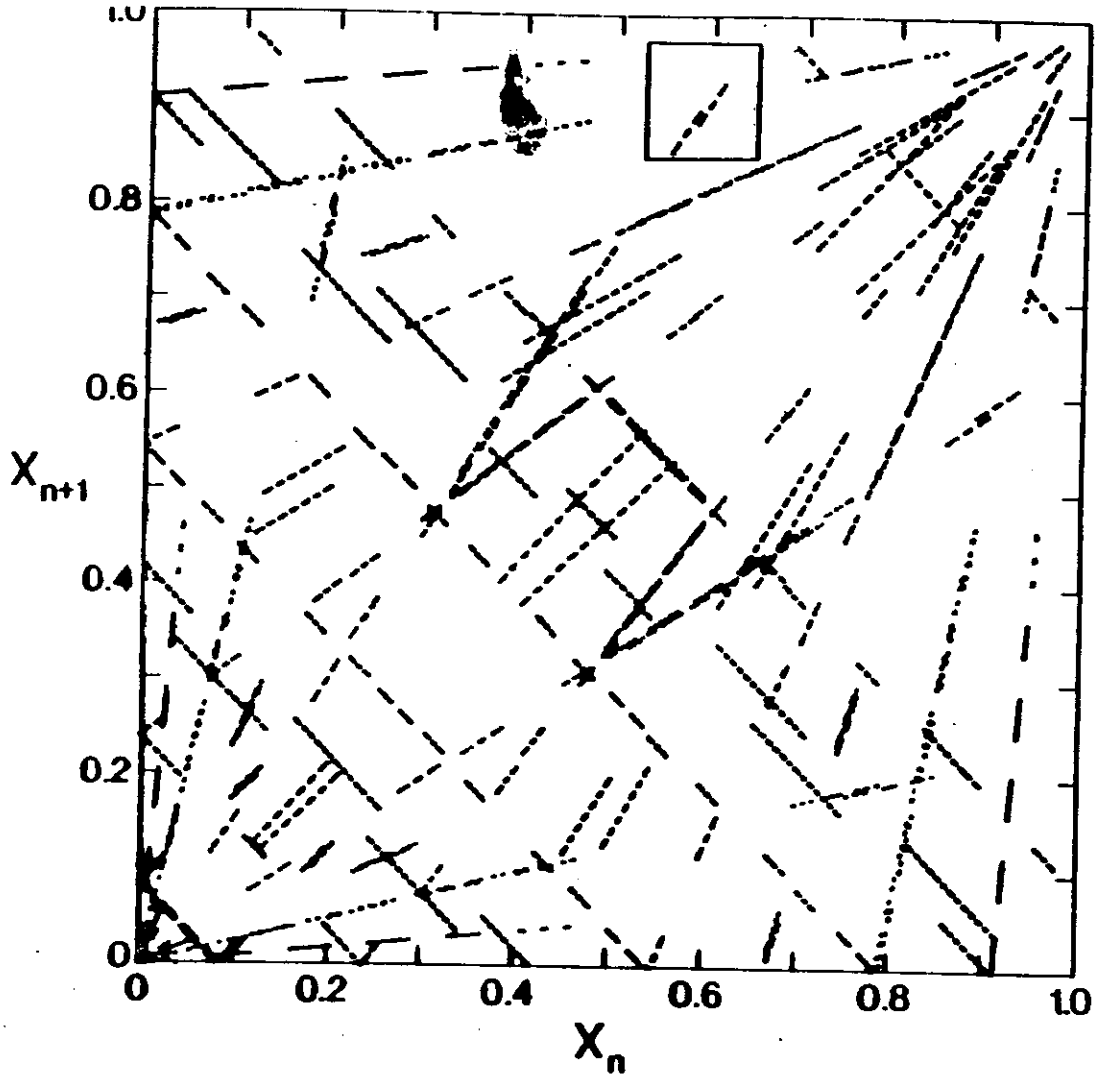
1.0
0.8
0.6
0.4
0.2
0
X_{n+1}
0
0.2
0.4
0.6
0.8
1.0
X_n

Fig. 4

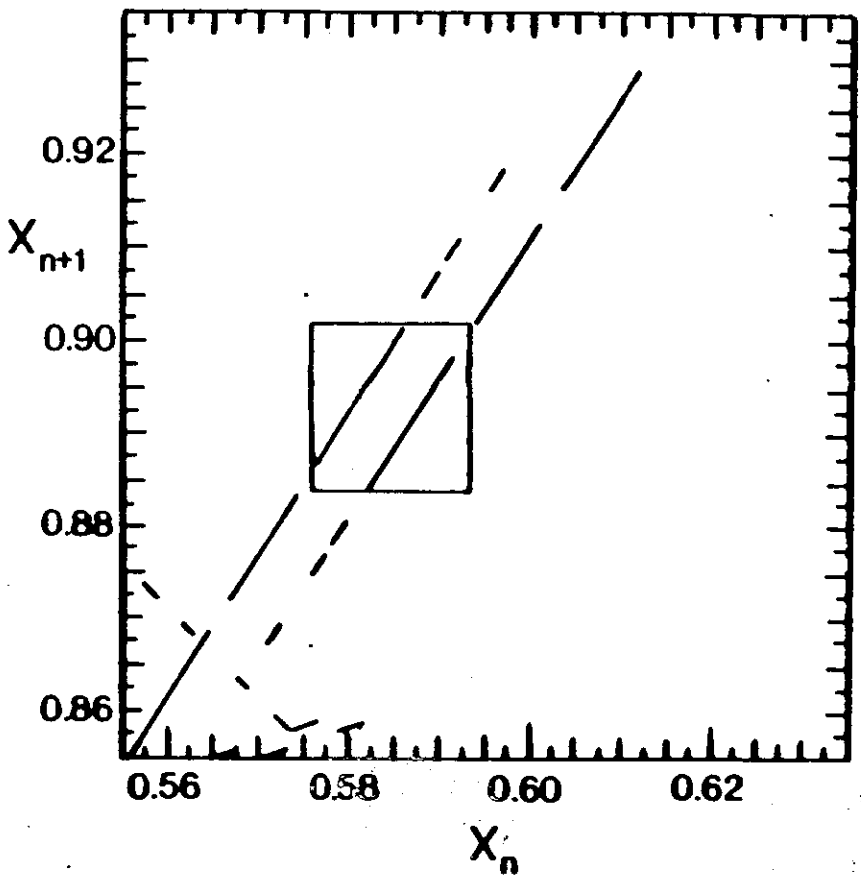
0.92
0.90
0.88
0.86
X_{n+1}
0.56
0.58
0.60
0.62
X_n

Fig. 5a

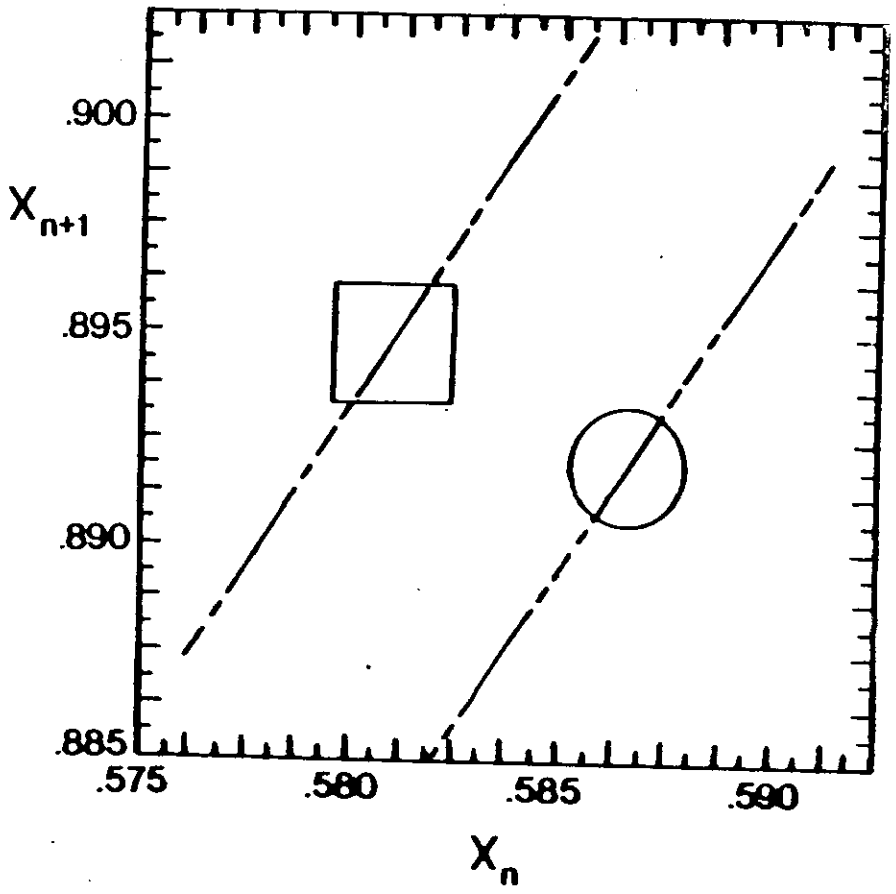
.900
.895
.890
.885
X_{n+1}
.575
.580
.585
.590
X_n

Fig. 5b

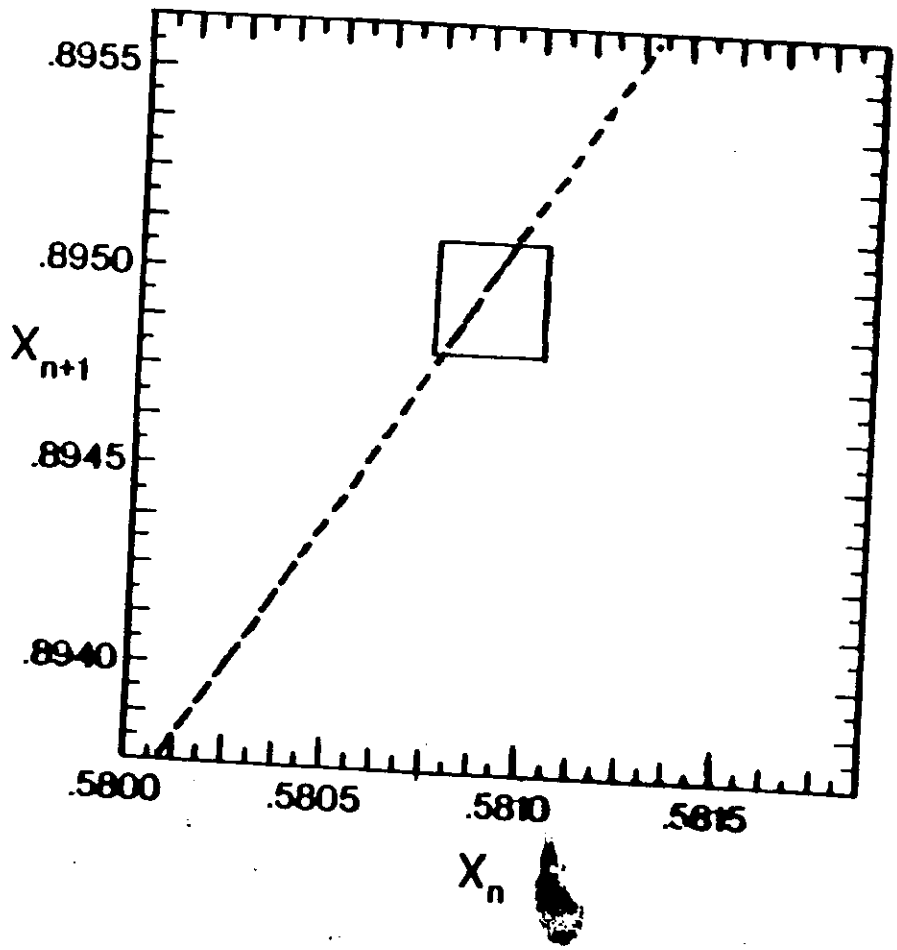
.8955
.8950
.8945
.8940
X_{n+1}
.5800
.5805
.5810
.5815
X_n

Fig. 5c

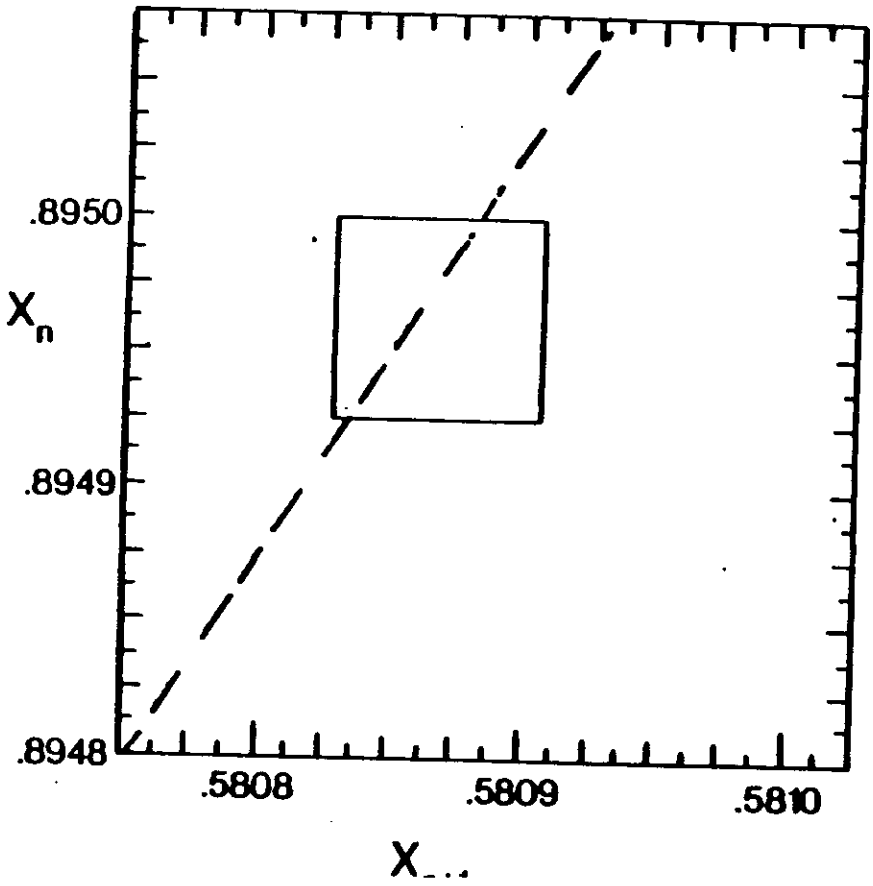
.8950
.8949
.8948
X_n
.5808
.5809
.5810
X_{n+1}

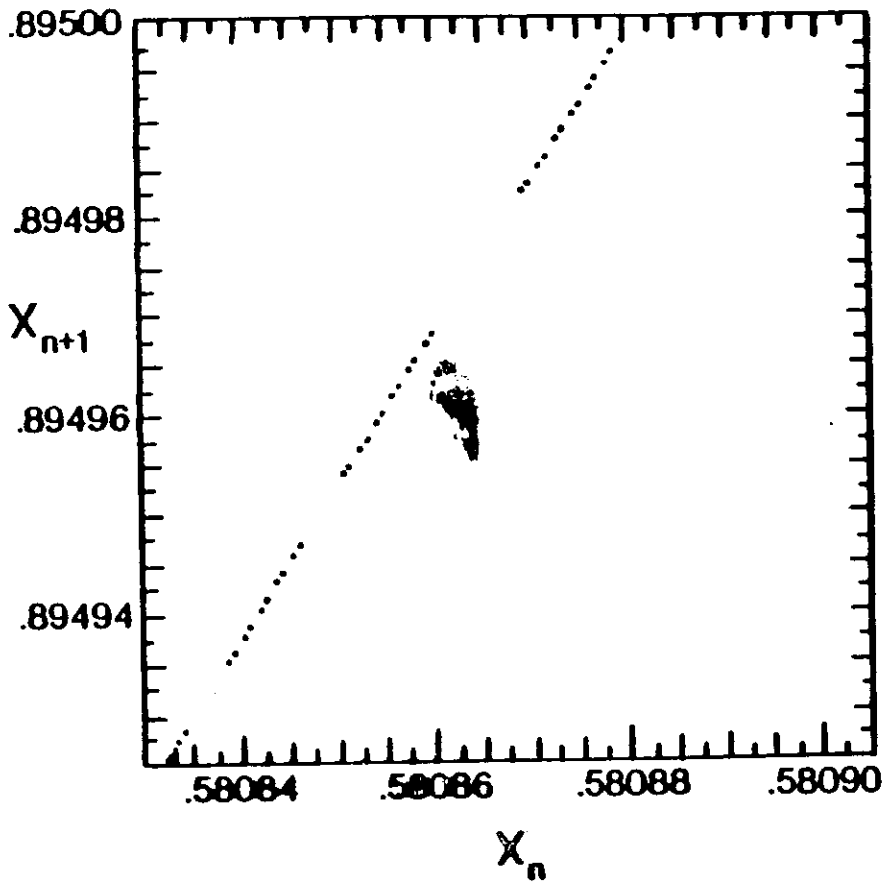
.89500
.89498
.89496
.89494
X_{n+1}
.58084
.58086
.58088
.58090
X_n

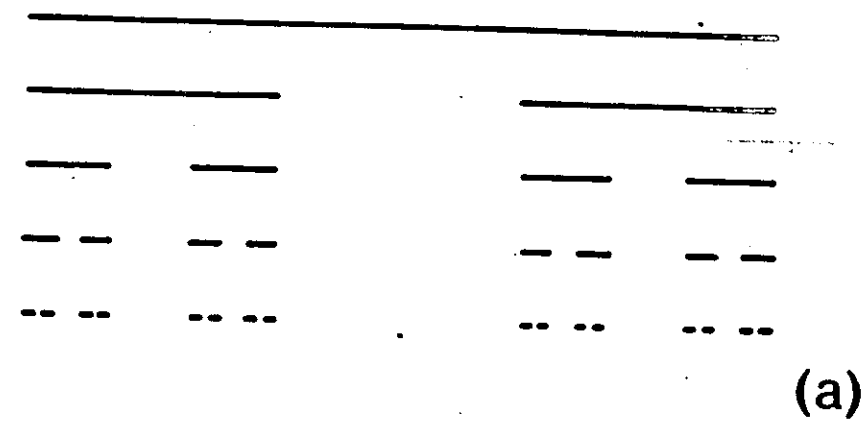
(a)

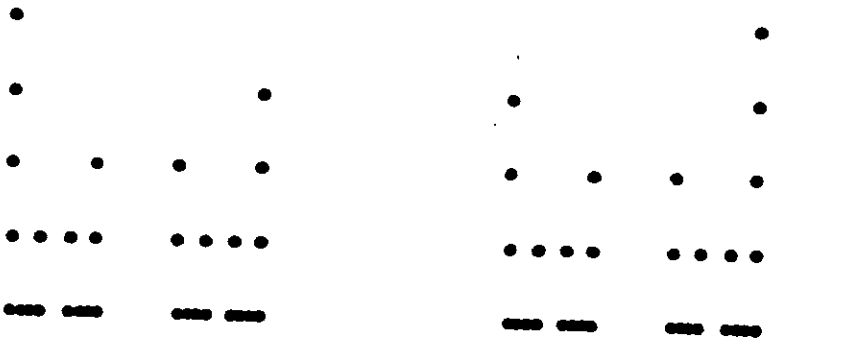
(b)

Fig. 6

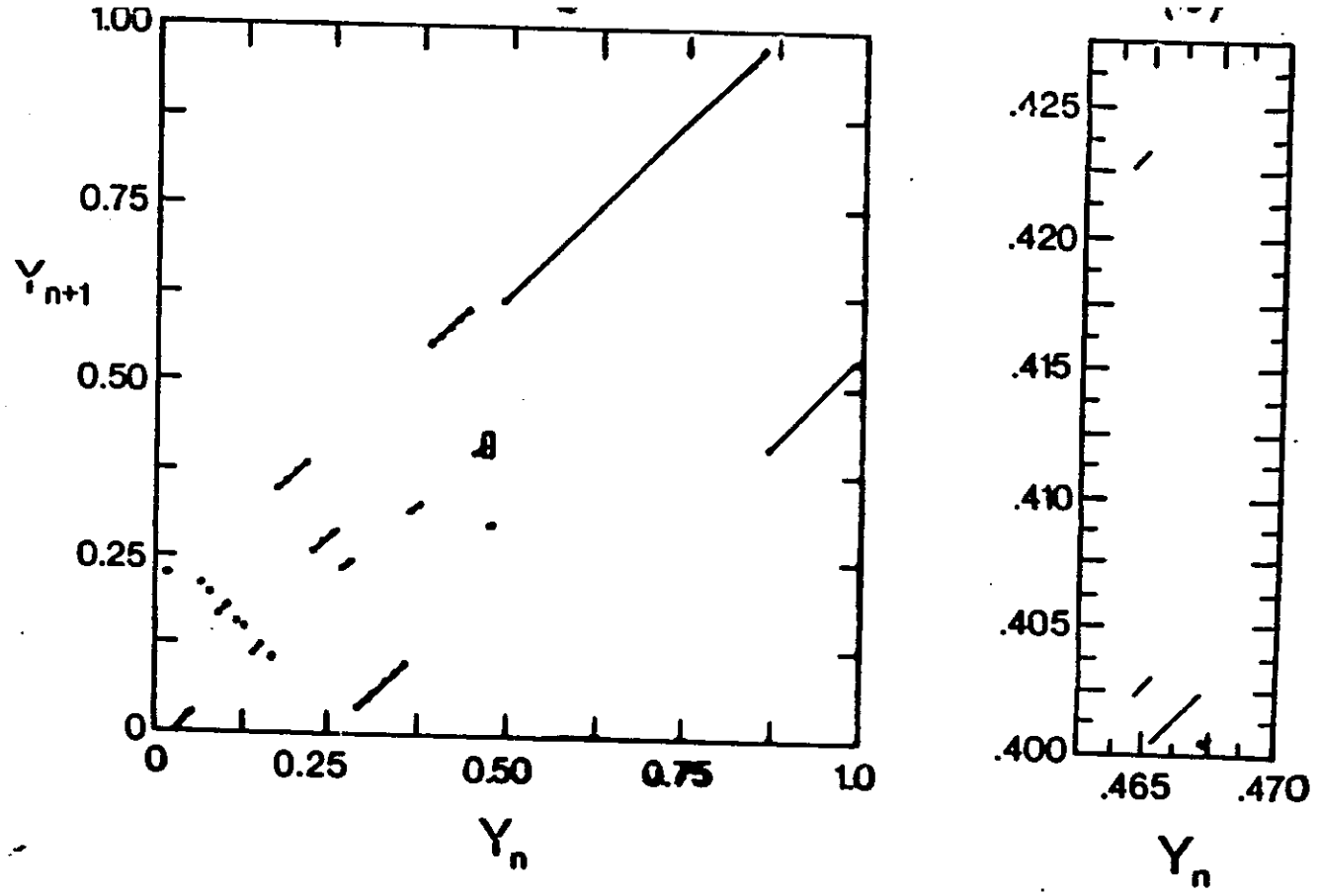
1.00
0.75
0.50
0.25
0
Y_{n+1}
0
0.25
0.50
0.75
1.0
Y_n
.425
.420
.415
.410
.405
.400
.465
.470
Y_n

Fig. 7

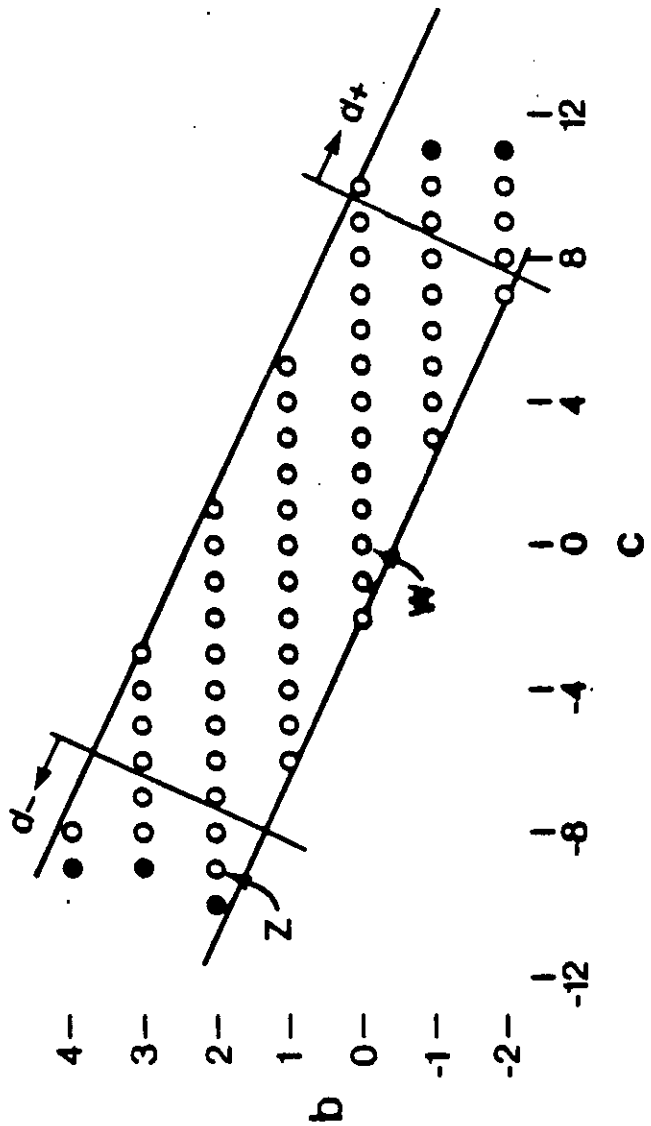
d+
d-
W
Z
12
8
4
0
-4
-8
-12
C
4
3
2
1
0
-1
-2
b

Fig. 8

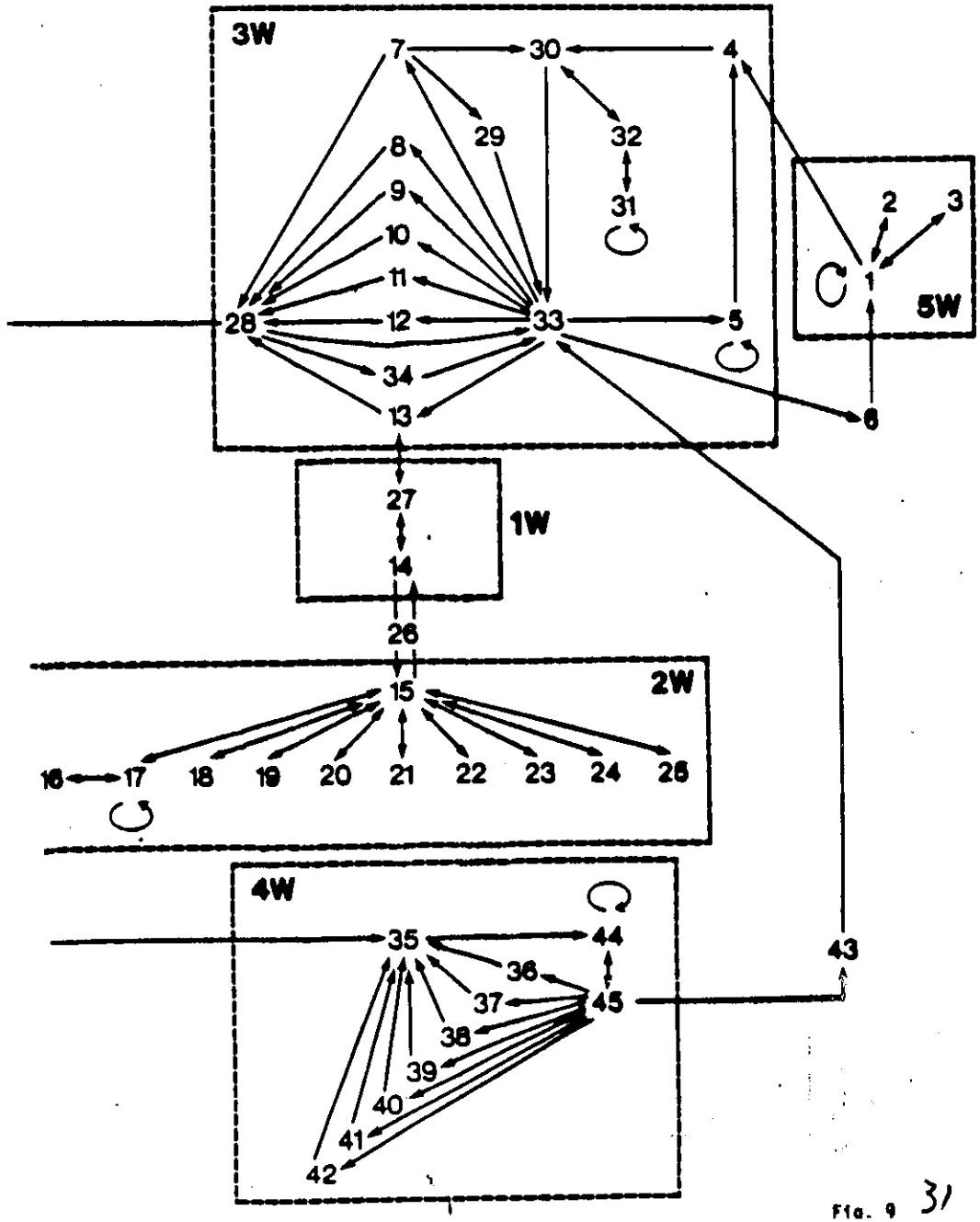
3W
7
30
4
29
32
8
9
31
10
11
2
3
28
12
33
5
1
5W
34
13
6
27
1W
14
26
2W
15
16
17
18
19
20
21
22
23
24
25
4W
35
44
36
43
37
45
38
39
40
41
42

Fig. 9

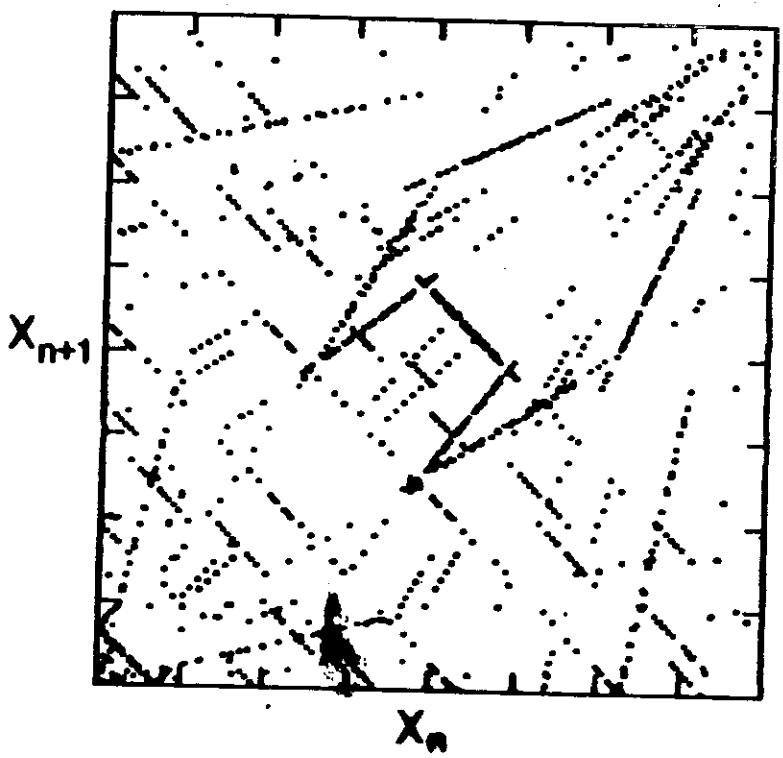

Fig. 10a

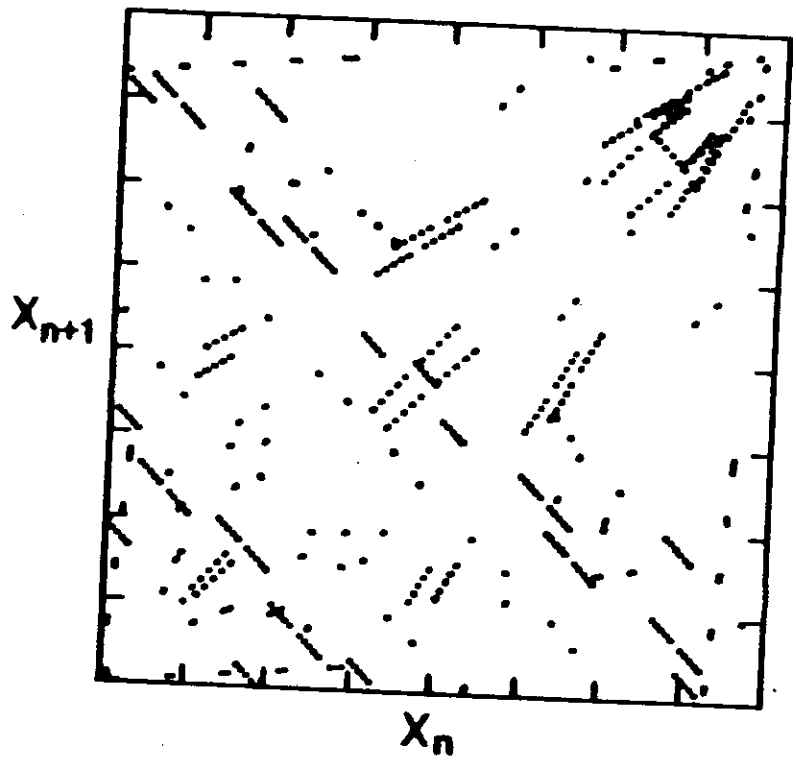

Fig. 10b

Bibliography for Knopoff Lectures.

K. Aki, Generation and propagation of G waves from the Niigata earthquake of June 16, 1964, part 2., Bull. Earthquake Res. Inst. Tokyo Univ., 44, 73-88, 1966.

R.E. Atkinson, Subcritical crack growth in geological materials, J. Struct. Geol., 4, 41-56, 1982.

J.N. Brune, Tectonic stress and the spectra of seismic shear waves from earthquakes, J. Geophys. Res., 75, 4997-5009, 1970.

R. Burridge and L. Knopoff, Model and theoretical seismicity, Bull. Seismol. Soc. Amer., 57 341-371, 1967.

N.L. Carter and M.C. Tsenn, Flow properties of continental lithosphere, Tectronophysics, 136, 27-63, 1987.

A.K. Chatterjee and L. Knopoff, Bilateral propagation of a spontaneous two-dimensional anti-plane shear crack under the influence of cohesion, Geophys. J. Roy. Astron. Soc., 73, 449-473, 1983.

Y.T. Chen and L. Knopoff, Static shear crack with a zone of slip-weakening, Geophys. J. Roy. Astron. Soc., 87, 1005-1024, 1986.

Y.T. Chen and L. Knopoff, The quasistatic extension of a shear crack in a viscoelastic medium, Geophys. J. Roy. Astron. Soc., 87, 1025-1039, 1986.

Y.T. Chen and L. Knopoff, Simulation of earthquake sequences, Geophys. J. Roy. Astron. Soc., 91, 693-709, 1987.

F.F. Evison, The precursory earthquake swarm, Nature, 266, 710-712, 1977.

M. Feigenbaum, Quantitative universality for a class of nonlinear transformations, J. Stat. Phys., 21, 25-52, 1978 .

M. Feigenbaum, The universal metric properties of nonlinear transformations, J. Stat. Phys., 21, 669-706, 1979.

J.K. Gardner and L.Knopoff, Is the sequence of earthquakes in Southern California, with aftershocks removed, Poissonian?, Bull. Seismol. Soc. Amer., 64, 1363-1367, 1974.

D.T. Griggs, Bull. Geol. Soc. Amer., 51, 1001-1002, 1940.

D.T. Griggs and J. Handin, Observations on fracture and a hypothesis of earthquakes, Geol. Soc. Amer., Mem. 79, 347-364, 1960.

R.H.G. Helleman, Self-generated chaotic behavior in nonlinear mechanics, in Fundamental Problems in Statistical Mechanics, Vol. 5, E.G.D. Cohen, ed., North Holland Publ., pp. 165-233, 1980.

M. Henon, A two-dimensional mapping with a strange attractor, Commun. Math. Phys., 50, 69-77, 1976.

M.K. Hubbert and W.W. Rubey, Role of fluid pressure in mechanics of overthrust faulting, Bull. Geol. Soc. Amer., 70, 1959.

L.M. Jones and P. Molnar, Some characteristics of foreshocks and their possible relationship to earthquake prediction and premonitory slip on faults, J. Geophys. Res., 84, 3596-3608, 1979.

Y.Y. Kagan, Spatial distribution of earthquakes: the four-point moment function, Geophys. J. Roy. Astron. Soc., 67, 719-733, 1981.

Y.Y. Kagan, Stochastic model of earthquake fault geometry, Geophys. J. Roy. Astron., Soc., 71, 659-691, 1982.

Y.Y. Kagan and L. Knopoff, Statistical search for non-random features of the seismicity of strong earthquakes, Phys.

Earth and Planet. Interiors, 12, 291-318, 1976.

Y.Y. Kagan and L. Knopoff, Earthquake risk prediction as a stochastic process, Phys. Earth and Planet. Interiors, 14, 97-108, 1977.

Y.Y. Kagan and L. Knopoff, Statistical study of the occurrence of shallow earthquakes, Geophys. J. Roy. Astron. Soc., 55, 67-86, 1978.

Y.Y. Kagan and L. Knopoff, Spatial distribution of earthquakes: the two-point correlation function, Geophys. J. Roy. Astron. Soc., 62, 303-320, 1980.

Y.Y. Kagan and L. Knopoff, Dependence of seismicity on depth, Bull. Seismol. Soc. Amer., 70, 1811-1822, 1980.

Y.Y. Kagan and L. Knopoff, Stochastic synthesis of earthquake catalogs, J. Geophys. Res., 86, 2853-2862, 1981.

Y.Y. Kagan and L. Knopoff, A stochastic model of earthquake occurrence, Proc. Eighth World Conf. on Earthquake Engineering, 1, 295-302, 1984 (Prentice-Hall, Inc., Englewood, N.J., Publishers).

Y.Y. Kagan and L. Knopoff, Statistical short-term earthquake prediction, Science, 236, 1563-1567, 1987.

V. Karnik, Seismicity of the European Area, Part 2, D. Reidel Publ. Co.

V.I. Keilis-Borok, Annali di Geofisica, 12, 1959.

V.I. Keilis-Borok, L. Knopoff, I.M. Rotvain and T.M. Sidorenko, Bursts of seismicity as long-term precursors of strong earthquakes, J. Geophys. Res., 85, 803-811, 1980.

V.I. Keilis-Borok, L. Knopoff, I.M. Rotwain and C.R. Allen, Intermediate-term prediction of occurrence times of strong earthquakes, Nature, 335, 690-694, 1988.

S.H. Kirby, Rheology of the lithosphere, Revs. Geophys. and Space Phys., 21, 1458-1487, 1983.

L. Knopoff, Energy release in earthquakes, Geophys. J. Roy. Astron. Soc., 1, 44-52, 1958.

L. Knopoff, The statistics of earthquakes in Southern California, Bull. Seismol. Soc. Amer., 54, 1871-1873, 1964.

L. Knopoff, A stochastic model for the occurrence of main sequence earthquakes, Revs. Geophys., 9, 175-188, 1971.

L. Knopoff and Y.Y. Kagan, Analysis of the theory of extremes as applied to earthquake problems, J. Geophys. Res., 82, 5647-5657, 1977.

L. Knopoff, Y.Y. Kagan and R. Knopoff, b-values for foreshocks and aftershocks in real and simulated earthquake sequences, Bull. Seismol. Soc. Amer., 72, 1663-1676, 1982.

L. Knopoff and V. Markushevich, Stationarity and stability of a Markov earthquake sequence, Computational Seismology, 16, 17-27, 1984. (English Version.)

L. Knopoff and J.O. Mouton, Can one determine seismic focal parameters from the far-field radiation? Geophys. J. Roy. Astron. Soc., 42, 591-606, 1975.

L. Knopoff and M.J. Randall, The compensated linear vector dipole, J. Geophys. Res., 75, 4957-4964, 1970.

L. Knopoff and W.I. Newman, Crack fusion as a model for repetitive seismicity, PAGEOPH, 121, 495-510, 1983.

B. Mandelbrot, The Fractal Geometry of Nature, W.H. Freeman, Publishers, 1982.

W.I. Newman and L. Knopoff, Crack fusion dynamics: A model for large earthquakes, Geophys. Res. Letts., 9, 735-738, 1982.

W.I. Newman and L. Knopoff, A model for repetitive cycles of large earthquakes, Geophys. Research Letts., 10, 305-308, 1983.
M. Ohnaka, Acoustic emission during creep of brittle rock, Intl. J. Rock Mech. Min. Sci. Geomech. Abstrs., 20, 121-134, 1983.
M. Ohtake, T. Matumoto and G. Latham, Seismic gap near Oaxaca, Southern Mexico, as a possible precursor to a large earthquake, PAGEOPH, 115, 375-385, 1977.
M. Ohtake, Search for precursors of the 1978 Izu-Hanto-Oki earthquake, Japan, PAGEOPH, 114, 1083-1093, 1976.
R. Page, Aftershocks and microaftershocks of the great Alaska earthquake of 1964, Bull. Seismol Soc. Amer., 58, 1131-1168, 1968.
D.N. Payton, R. Rich, W.M. Visscher, Physical Review, 160, 129, 1967.
C.F. Richter, Elementary Seismology, W.H. Freeman and Co., Publishers, 1958.
T.J. Rolfe. S.A. Rice,and J. Dancz, J. Chem. Phys., 70, 26, 1979.
N. Saito, N. Ooyama, T. Aizawa,and H. Hirooka, Prog. Theor. Phys. Suppl., 45, 209, 1970.
P. Segall and D.D. Pollard, Mechanics of discontinuous faults, J. Geophys. Res., 85, 4337-4350, 1980.
P. Segall and D.D. Pollard, Joint formation in granitic rock of the Sierra Nevada, Geol. Soc. Amer. Bull., 94, 563-575, 1983.
W. Thatcher and T.C. Hanks, Source Parameters of Southern California Earthquakes, J. Geophys. Research, 78, 8547-8576, 1973.
J.M.T. Thompson and H.B. Stewart, Nonlinear Dynamics and Chaos, John Wiley and Sons, Publishers, 1986.
M. Toda, Theory of Nonlinear Lattices, Springer Verlag, [redacted], 1981.
M.Toda, Proc. Phys. Soc. Japan, 23, 501, 1967.
M.C. Tsenn and N.L. Carter, Upper limits of power law creep of rocks, Tectonophysics, 136, 1-26, 1987.
T. Yamashita and L. Knopoff, Models of aftershock occurrence, Geophys. J. Roy. Astron. Soc., 91, 13-26, 1987.
N.J. Zabusky and M. D. Kruskal, Interaction of solitons in a collisionless plasma and the recurrence of initial states, Phys. Rev. Letts., 165, 240-243, 1965.

Note @ This bibliography should be included with the general bibliography of the whole [redacted]

@ [redacted]

ADDITIONAL BIBLIOGRAPHY [redacted]

1. M.E. Fisher, The renormalization group in the theory of critical behavior,
Rev. Mod. Phys. (1974), vol. 46, no. 4, pp. 597-615.

2. L.P. Kadanoff, Scaling laws for Ising models near T_c,
Physics (N.Y.) (1966) vol. 2, no. 6, pp. 263-272.

3. K.G. Wilson, Renormalization group and critical phenomena, I. Renormalization group and the Kadanoff scaling picture.
Phys. Rev. B, (1971), vol. 4, no. 9, pp. 3174-3183.

4. Th. Niemeyer, J.M.J. van Leeuven, Wilson theory for 2-dimensional Ising spin systems,
Physica (1974), vol. 71, pp. 17-40.

5. L.P. Kadanoff, A. Houghton, Numerical evaluations of the critical properties of the 2-dimensional Ising model,
Phys. Rev. B (1975), vol. 11, no. 1, pp. 377-386.

6. K.G. Wilson, J. Kogut, The renormalization group and the ε expansion,
Phys. Rep. (1974), vol. 12, pp. 75-200.

7. M. Suzuki, K. Sogo, I. Matsuba, H. Ikeda, T. Chikama, H. Takano, Real-space renormalization group approach to critical dynamics,
Prog. Theor. Phys. (1979), vol. 61, no. 3, pp. 864-880.

8. Y. Achiam, A real space time-dependent renormalization group of the one-dimensional Ising model,
J. Phys. A: Math. Gen. (1978), vol. 11, no. 5, pp. 975-981.

9. S.K. Ma, Renormalization group by Monte Carlo methods,
Phys. Rev. Lett. (1976), vol. 37, no. 8, pp. 461-464.

10. J. Tobochnik, S. Sarker, R. Cordery, Dynamic Monte Carlo renormalization group,
Phys. Rev. Lett. (1981), vol. 46, no. 21, pp. 1417-1420.

11. N. Jan, L.L. Moseley, D. Stauffer, Dynamic Monte Carlo Renormalization group,
J. Stat. Phys. (1983), vol. 33, no. 1, pp. 1-11.

12. R.F. Smalley Jr., D.L. Turcotte, S.A. Solla, A renormalization group model for the stick-slip behavior of faults,
J. Geoph. Res. (1985), vol. 90, no. B2, pp. 1894

13. C.J. Allegre, J.L. LeMouel, A. Provost, Scaling rules in rock fracture and possible implications for earthquake prediction.
Nature (1982), vol. 297, pp. 47-49.

14. V.C. Li and C. Kisslinger, Stress transfer and nonlinear stress accumulation at subduction plate boundaries - Application to the Aleutians, PAGEOPH, 122, 812-830, 1984/85.

15. C.A. Morrow, L.Q. Shi and J.D. Byerlee, Permeability of fault gouge under confining pressure and shear stress, J. Geophys. Res., 89, 3193-3200, 1984.

16. E. Guyon, J.-P. Hulin, and R. Lenormand, Application de la percolation à la physique des milieux poreux, Annales des Mines, May-June 1984, pp. 17-40.